Host ZCCHC3 blocks HIV-1 infection and production by a dual mechanism

Binbin Yi[1], Yuri L Tanaka[2], Hidetaka Kosako[3], Erika P Butlertanaka[2], Prabuddha Sengupta[4], Jennifer Lippincott-Schwartz[4], Akatsuki Saito[2,5,6*†] and Shige H. Yoshimura[1*†]

[1] Graduate School of Biostudies, Kyoto University, Yoshida-Konoe-Cho, Sakyo-ku, Kyoto, 606-8501, Japan

[2] Department of Veterinary Medicine, Faculty of Agriculture, University of Miyazaki, 1-1 Gakuen Kibanadai-nishi, Miyazaki, Miyazaki, 889-2192, Japan

[3] Division of Cell Signaling, Fujii Memorial Institute of Medical Sciences, Institute of Advanced Medical Sciences, Tokushima University, 3-18-15 Kuramoto-cho, Tokushima, 770-8503, Japan

[4] Howard Hughes Medical Institute, Janelia Research Campus, 19700 Helix Drive, Ashburn, VA 20147, U.S.A.

[5] Center for Animal Disease Control, University of Miyazaki, 1-1 Gakuen Kibanadai-nishi, Miyazaki, Miyazaki, 889-2192, Japan

[6] Graduate School of Medicine and Veterinary Medicine, University of Miyazaki, 5200 Kiyotakecho Kihara, Miyazaki, Miyazaki, 889-1692, Japan

* corresponding authors

† These authors contributed equally to this work.

Most mammalian cells prevent viral infection and proliferation by expressing various restriction factors and sensors that activate the immune system. While anti-human immunodeficiency virus type 1 (HIV-1) host restriction factors have been identified, most of them are antagonized by viral proteins. This has severely hindered their development in anti-HIV-1 therapy. Here, we describe CCHC-type zinc-finger-containing protein 3 (ZCCHC3) as a novel anti-HIV-1 factor that is not antagonized by viral proteins. ZCCHC3 suppresses production of HIV-1 and other retroviruses. We show that ZCCHC3 acts by binding to Gag nucleocapsid protein via zinc-finger motifs. This prevents interaction between the Gag nucleocapsid protein and viral genome and results in production of genome-deficient virions. ZCCHC3 also binds to the long terminal repeat on the viral genome via the middle-folded domain, sequestering the viral genome to P-bodies, which leads to decreased viral replication and production. Such a dual antiviral mechanism is distinct from that of any other known host restriction factors. Therefore, ZCCHC3 is a novel potential target in anti-HIV-1 therapy.

33 Human immunodeficiency virus type 1 (HIV-1) infection is a major health concern, affecting tens of
34 millions of individuals worldwide. The life cycle of the human immunodeficiency virus (HIV-1)
35 largely relies on a large number of host proteins that promote efficient progress of viral replication,
36 packaging, and budding. As a defence strategy, host cells produce a number of restriction factors, i.e.,
37 proteins that prevent a specific step in the viral life cycle or recognize specific viral components and
38 activate the immune system[1,2]. Several anti-HIV-1 restriction factors have been identified and
39 investigated to date[3]. Their antiviral mechanism involves interaction with, modification of, and/or
40 blocking of specific viral structures. For instance, some host factors target the viral genome. An
41 example is the APOBEC3[4–6] family proteins that inhibit viral proliferation by introducing nucleotide
42 mutations in the viral genome during its reverse transcription[8,9]. Another protein, ZAP1[10,11], recognizes
43 single-stranded CG dinucleotide-rich regions of HIV-1 RNA[12,13] and recruits a ribonuclease and RNA
44 exosome to degrade it. As another example, the nuclear exosome-targeting (NEXT) complex
45 recognizes the transactivation response (TAR) element on the HIV-1 genome and inhibits
46 transcription[14]. Other host factors target viral proteins. For instance, tetherin anchors the HIV-1 particle
47 to the host plasma membrane and prevents the release of the virion into the extracellular space[18,19].
48 SAMHD1 prevents the reverse transcription of HIV-1 by depleting the intracellular dNTP pool[20,21].
49 All these restriction factors stimulate various innate immune responses, such as induction of type I
50 interferons (IFNs) and other pro-inflammatory cytokines, triggering ubiquitin-mediated
51 proteolysis[24,25]. In response, HIV-1 utilizes viral accessory proteins to evade inhibition by the
52 restriction factors. For example, the HIV-1 protein Vif antagonizes the antiviral activity of APOBEC3[6],
53 and the HIV-1 protein Vpu antagonizes the antiviral activity of tetherin[17,18]. Host factors that inhibit
54 broad HIV-1 strains and other retroviruses but are not antagonized by viral proteins are potential
55 attractive therapeutic targets. However, no such factors, especially that target multiple steps of HIV-1
56 replication, have been identified to date.
57 CCHC-type zinc-finger-containing protein 3 (ZCCHC3; [NP_149080.2]) is a host factor with a

58 potential antiviral activity. It was initially identified by an interactome analysis on the basis of its
59 interaction with HIV-1 Gag[26] and was eventually shown to regulate the activity of the interferon-
60 stimulated response gene (ISG), which reduced the virus replication by degrading viral RNA[27]. It
61 functionally interacts with cGAS[28], RIG-I[29], and TLR3[30], major cytoplasmic nucleic acid sensors that
62 activate the innate immune signalling pathway. ZCCHC3 acts together with cGAS to recognize
63 double-stranded (ds) DNA and with RIG-I and TLR3 to recognize dsRNA, although no direct physical
64 interaction between ZCCHC3 and these proteins has been reported. Porcine ZCCHC3 also suppresses
65 the replication of the pseudorabies virus by activating the IFN-β expression[30,31]. Despite the
66 accumulating evidence of the antiviral role of ZCCHC3, its functional involvement in the HIV-1 life
67 cycle remains elusive. Elucidation of ZCCHC3's potent anti-HIV-1 activity could contribute to
68 developing novel therapeutic strategies. Accordingly, in this study, we investigated the interaction
69 between ZCCHC3 and HIV-1 in detail.
70
71 ***ZCCHC3 and retroviral infectivity***
72 We first confirmed that ZCCHC3 is expressed in a wide variety of cell types, including epithelial cells
73 and monocytes (Fig. 1a). To examine the effect of ZCCHC3 on HIV-1, we transfected Lenti-X 293T
74 cells with pNL4-3 plasmid, which is most widely used for generating an infectious HIV-1NL4-3 strain,
75 with or without a plasmid encoding human influenza hemagglutinin (HA)-tagged human ZCCHC3
76 (Fig. 1b). Human ZCCHC3 cDNA was used in all experiments unless indicated otherwise. We then
77 harvested the released virions and tested their infectivity on TZM-bl cells. TZM-bl is a reporter cell
78 line that expresses a luciferase reporter protein, and the expression level of luciferase depends on the
79 viral Tat protein[32-37]. While we observed a clear cytopathic effect with the NL4-3-infected TZM-bl
80 cells (Extended Data Fig. 1a, bottom right panel), the morphological changes of cells infected with the
81 NL4-3 virus produced in the presence of ZCCHC3 were negligible (Extended Data Fig. 1a, bottom
82 left panel). Further, the measurement of luciferase activity in TZM-bl cells demonstrated that the

83 overexpression of ZCCHC3 reduced the infectivity of HIV-1 (NL4-3) by two orders of magnitude (Fig.
84 1c), supporting the initial observation. We observed a similar effect with various HIV-1 strains, HIV-
85 2, and simian immunodeficiency virus in chimpanzees (SIVcpz), although the extent of suppression
86 varied among the strains (Fig. 1c). Specifically, one of the transmitted/founder (TF) HIV-1 strains,
87 TF2625 strain, showed higher sensitivity to ZCCHC3 suppression than the TF2626 strain (p=0.0002),
88 suggesting that susceptibility to ZCCHC3 differs between viral strains. Collectively, ZCCHC3
89 strongly suppresses HIV-1 infectivity.
90 HIV-1 enters target cells via a fusion between viral Envelope (Env) and cellular membrane. To test
91 whether the antiviral effect of ZCCHC3 is HIV-1 Env-dependent, we used a Δ*env* HIV-1 pMSMnG
92 construct, which is pseudotyped with a VSV-G envelope, which utilizes a clathrin-mediated endocytic
93 route to enter into cells[38]. We observed an antiviral effect of ZCCHC3 similar to that seen in the initial
94 experiment, indicating that the antiviral effect of ZCCHC3 is HIV-1 Env-independent (Extended Data
95 Fig. 1b). While we observed comparable antiviral inhibition by ZCCHC3 in TZM-bl and $CD4^+$ T cell-
96 derived C8166-CCR5 cells, the inhibitory effect was relatively more pronounced in THP-1 cells
97 (Extended Data Fig. 1b), suggesting that the antiviral effect of ZCCHC3 depends on the target cell
98 type. In addition to WT HIV-1, we tested two HIV-1 Gag capsid (CA) mutants that cannot interact
99 with CPSF6 (N74D)[39] or CypA (RGDA/Q112)[40]. Previous studies demonstrated that CPSF6[39] and
100 CypA[41] are both involved in the early steps of HIV-1 replication, including reverse transcription,
101 uncoating, nuclear entry, and integration targeting of proviral DNA (reviewed in [42]). While WT and
102 N74D viruses showed comparable sensitivity to ZCCHC3, the RGDA/Q112D virus was slightly more
103 resistant to suppression than WT and N74D viruses (Extended Data Fig. 1c). This suggested that CA
104 sequence may affect the susceptibility of HIV-1 to ZCCHC3.
105 Further, we observed that ZCCHC3 suppresses the infectivity of an HIV-1–based lentiviral vector,
106 psPAX2-IN/HiBiT, that lacks accessory proteins, such as Vif, Vpu, Vpr, and Nef, to an extent similar
107 to that of HIV-1 (compare Fig. 1c and Fig. 1d). This indicated that the inhibitory effect of ZCCHC3 is

108 not antagonized by the accessory proteins. Notably, ZCCHC3 also suppressed the infection of other
109 retroviruses, such as the simian immunodeficiency virus of macaques (SIVmac), feline
110 immunodeficiency virus (FIV), equine infectious anaemia virus (EIAV), and murine leukaemia virus
111 (MLV) (Fig. 1d), suggesting that ZCCHC3 inhibits the infection of a broad range of retroviruses. The
112 suppression effect was proportional to the amount of ZCCHC3 plasmid used for viral production
113 (Extended Data Fig. 1d). Further, *ZCCHC3* knockdown with siRNA (Extended Data Fig. 1e) and
114 *ZCCHC3* knockout (Extended Data Fig. 1f) slightly increased lentiviral infectivity (Fig. 1e, Extended
115 Data Fig. 1g,h). In addition, ZCCHC3 protein from different species (Extended Data Fig. 1i,j)
116 suppressed the infectivity of JRCSF and TF2625 strains to a level similar to that of human ZCCHC3
117 (Extended Data Fig. 1j). The TF2626 strain was relatively resistant to ZCCHC3 from animals. The
118 TF2625 strain, which exhibited higher sensitivity to human ZCCHC3 than TF2626 (Fig. 1c), was also
119 more sensitive to ZCCHC3 proteins from other species tested than the TF2626 strain (Extended Data
120 Fig. 1j). These observations suggested that the antiretroviral activity is conserved in mammals.
121 Together, these results indicated that ZCCHC3 suppresses the infectivity of HIV-1 and other
122 retroviruses.

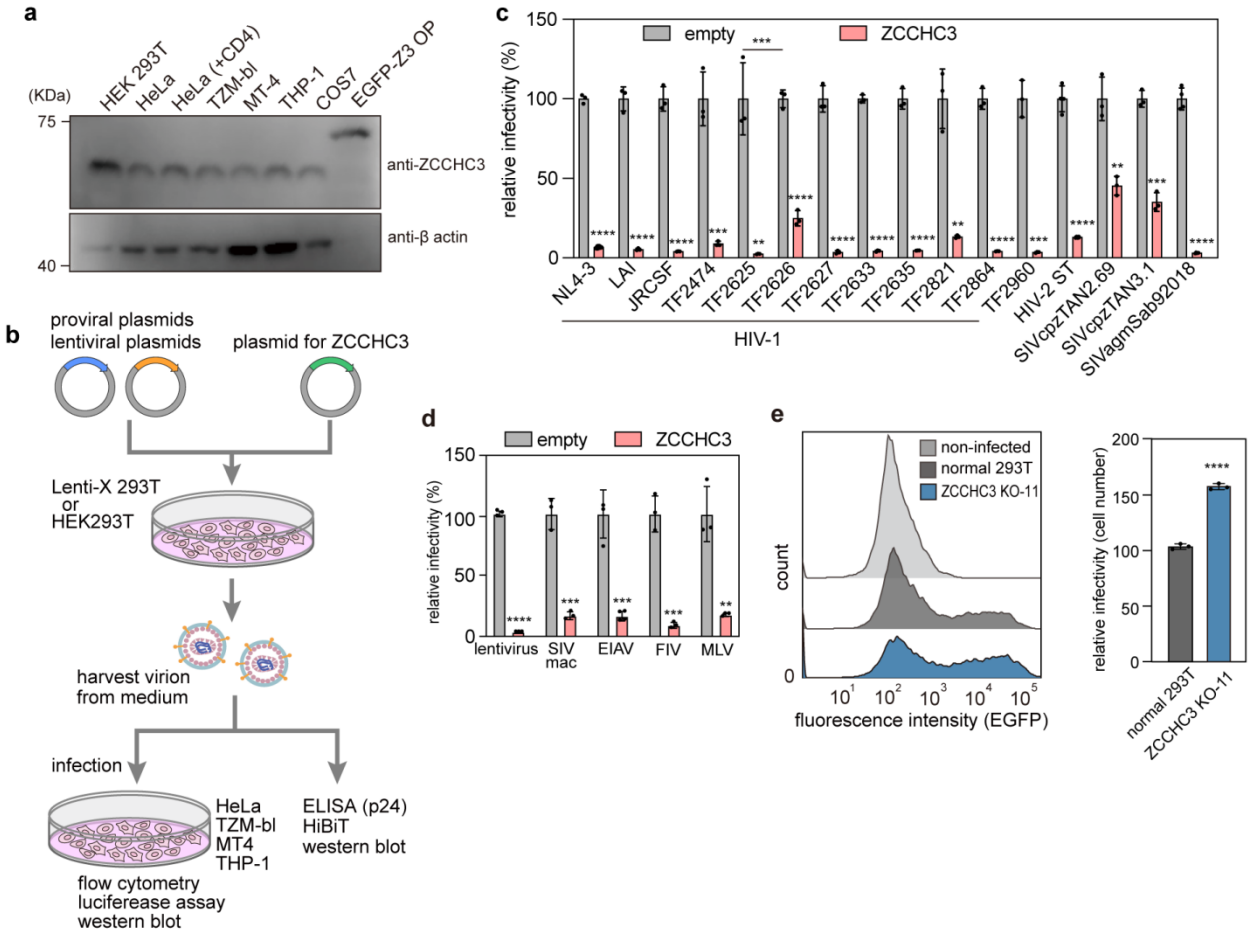

Fig. 1| Effect of ZCCHC3 on viral infection. a, ZCCHC3 expression in different cell types, determined in cell lysates by western blotting with an anti-ZCCHC3 antibody. HEK293T cells expressing EGFP-tagged ZCCHC3 were the positive control. The control lane contained five times less lysate than the other lanes. The panel shown here is a representative image of three independent experiments. **b**, Experimental flow overview for panels in Figures 1 and 2. Producer cells (HEK293T or Lenti-X 293T) were transfected with viral plasmids and a ZCCHC3 expression plasmid, and the virions were collected from the culture medium and then analyzed as indicated. **c**, Effect of ZCCHC3 on the infectivity of various viral strains. Plasmids encoding individual viral strains were introduced into Lenti-X 293T cells in the presence or absence of a HA-ZCCHC3 expression plasmid. Culture supernatant was collected 2 days after transfection and used to infect TZM-bl cells. Infectivity was determined as relative light units of luciferase 2 days after infection. The mean and standard deviation values are shown (n = 3). **d**, Effect of ZCCHC3 on viral infectivity of retroviral vectors. A plasmid encoding the indicated retrovirus and luciferase reporter gene was introduced into Lenti-X 293T cells with or without a HA-ZCCHC3 expression plasmid. Culture supernatant was collected 2 days after transfection and used to infect MT-4 cells. Infectivity was determined as in (**c**). Values relative to those for cells harbouring empty vector are shown as the mean ± standard deviation. **e**, Effect of ZCCHC3 knockout on viral production. Lentiviruses produced in WT and ZCCHC3-knockout Lenti-X 293T cells were normalized to p24 and used to infect HeLa cells. The expression of a viral gene (EGFP) was assessed by flow cytometry (left). EGFP-positive cells were quantified (right); the mean and standard deviation values are shown (n = 3). Differences were examined by a two-tailed, unpaired Student's *t*-test; ****$p < 0.0001$, ***$p < 0.001$, **$p < 0.01$. In panel c, difference between TF2625 and TF2626 was examined by one-way ANOVA, followed by Tukey's test; ***$p < 0.001$.

144 ***ZCCHC3 and viral production***

145 We next assessed if ZCCHC3 decreased HIV-1 infectivity by affecting viral production. Accordingly,
146 we quantified virions released from pNL4-3-transfected Lenti-X 293T cells into the culture medium
147 by enzyme-linked immunosorbent assay (ELISA) of viral p24 protein. Co-expression of ZCCHC3
148 with HIV-1 proviral plasmids reduced the production of virions by all the viruses tested (Fig. 2a). The
149 production was increased by 72% upon *ZCCHC3* knockout (Extended Data Fig. 2a, KO-11), and the
150 effect was dependent on the amount of ZCCHC3 (Extended Data Fig. 2b). Western blot analysis
151 revealed that the reduced viral production was caused by the reduction of viral protein (Gag) in the
152 producer cells (Fig. 2b). In addition, we found that ZCCHC3 affected the processing of Gag (Fig. 2b,
153 Extended Data Fig. 2c). Specifically, co-expression of ZCCHC3 increased the amount of p49 and p41.
154 Together, ZCCHC3 reduced the production of virions by inducing decreased Gag expression and
155 abnormal Gag processing.

156 To test whether the inhibition of infection was caused by the reduced virion production, we infected
157 TZM-bl cells with a p24-normalized virion load. Notably, NL4-3 virions produced by ZCCHC3-
158 overexpressing Lenti-X 293T cells showed lower infectivity than those produced by non-ZCCHC3-
159 overexpressing cells (Fig. 2c). This suggested that virions produced in the presence of ZCCHC3 are
160 defective and have reduced infectivity. Next, to start dissecting the underlying mechanism, we
161 analyzed the amount of viral RNA in virions. We harvested lentiviruses produced by 293T cells in the
162 absence or presence of ZCCHC3 overexpression, and analyzed the p24-normalized virion load by
163 reverse transcription quantitative polymerase chain reaction (RT-qPCR). Indeed, the amount of viral
164 RNA in the virions was greatly reduced upon ZCCHC3 co-expression (Fig. 2d). Together, these results
165 indicated that ZCCHC3 inhibits the production of infectious virus particles by both, reducing Gag
166 expression and inhibiting the packaging of viral RNA.

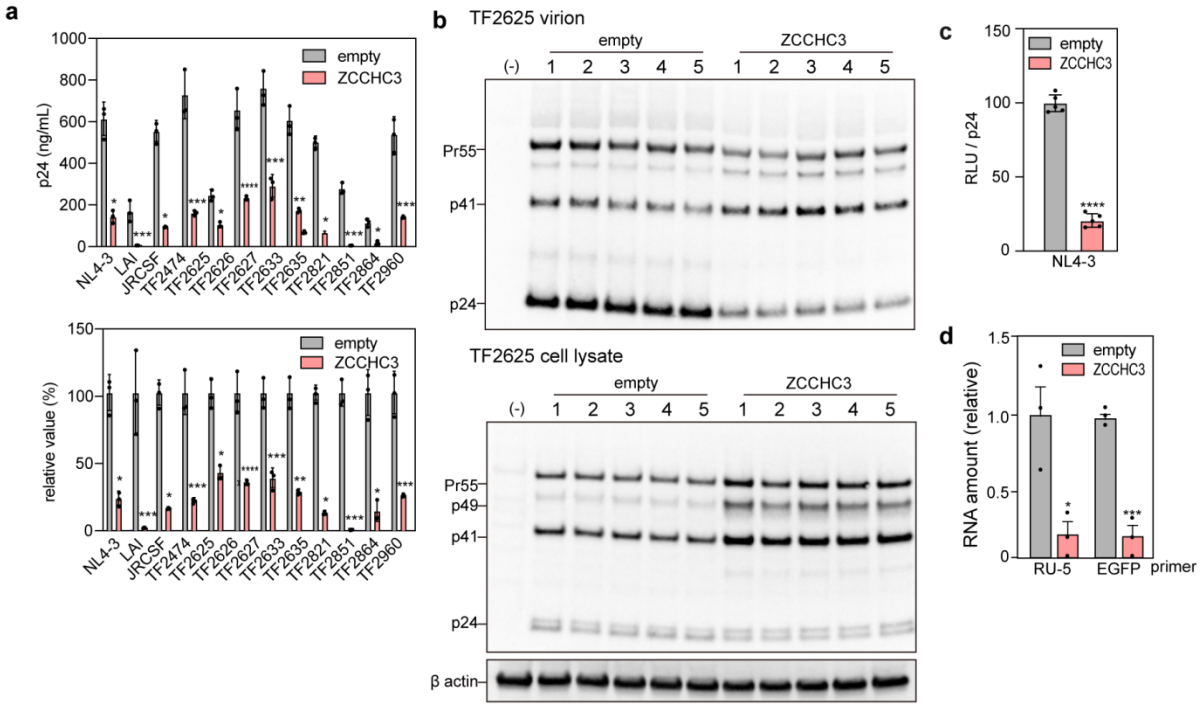

Fig. 2| Effect of ZCCHC3 on viral production. **a**, Effect of ZCCHC3 on HIV-1 viral production. A plasmid encoding HA-tagged ZCCHC3 or empty HA-vector was introduced into Lenti-X 293T cells together with an HIV-1-encoding plasmid. Virions released into the culture medium were quantified by p24 ELISA. The absolute value (left) and the value relative to that without ZCCHC3 (right) are shown (n = 3). **b**, ZCCHC3 affects the Gag processing. Lenti-X 293T cells were co-transfected with pTF2625 plasmids in the presence or absence of HA-ZCCHC3. Equal volume of the pelleted virions and cell lysates were analyzed by western blotting using an anti-p24 antibody. The quantification of the band intensity is shown in Extended Data Fig. 2c. For cell lysate analysis, the membrane was re-probed with an anti-β-actin antibody as a loading control (n = 5). **c**, Effect of ZCCHC3 on infectivity of ZCCHC3-loaded virions. TZM-bl cells were infected with the same amount (p24-normalized) of NL4-3 or lentivirus with or without ZCCHC3 in the virion. Infectivity was analyzed by luciferase assay and is presented relative to that without ZCCHC3 as the mean and standard deviation (n = 5). **d**, Effect of ZCCHC3 co-expression on lentivirus production. HEK293T cells were transfected with lentiviral plasmids (pLV-EGFP, psPAX2, pMD2.G) with or without a HA-ZCCHC3 expression plasmid. Total RNA was purified from lentiviruses harvested from the culture medium and analyzed by RT-qPCR. The mean and standard deviation values are shown (n = 3). In panels **a**, **c, d**, differences were examined by a two-tailed, unpaired Student's *t*-test; ****$p < 0.0001$, ***$p < 0.001$, **$p < 0.001$, *$p < 0.05$.

ZCCHC3 domains for GagNC–RNA binding

The described experiments suggested that ZCCHC3 directly interacts with Gag and/or viral genomic RNA. To test this, we performed a pull-down assay with different glutathione *S*-transferase (GST)-tagged Gag fragments: matrix (MAp17), capsid (CAp24), nucleocapsid (NCp7), and p6. The experiment revealed that ZCCHC3 bound to HIV-1 NCp7 and MLV GagNC (Fig. 3a). In good

189 agreement with this, we detected ZCCHC3 in virions released into the culture medium by Lenti-X
190 293T cells (Fig. 3b). In fact, ZCCHC3 was present not only in TF2625 virions (Fig. 3b), but also in
191 lentiviral virions and virus-like particles (VLPs) produced by HIV-1 Gag in the absence of other viral
192 components (Fig. 3c). Subsequent analysis of COS7 cells expressing HA-ZCCHC3 or enhanced green
193 fluorescent protein (EGFP)-fused ZCCHC3 and Gag-mCherry confirmed that ZCCHC3 colocalized
194 with Gag signal both inside the producer cell and in the released VLPs (Fig. 3d). This demonstrated
195 that a direct interaction between ZCCHC3 and GagNC is sufficient for the incorporation of ZCCHC3
196 into the virion.
197 We next assessed which ZCCHC3 domain is involved in the interaction with GagNC. ZCCHC3 is
198 composed of an N-terminal intrinsically disordered region (IDR), middle fold (MF) domain, and three
199 C-terminal tandem repeats of CCHC-type zinc-finger motifs (ZnF) (Fig. 4a). We expressed these
200 fragments in HEK293T cells and quantified the viral production and infectivity. We observed that
201 ZCCHC3 IDR (N) did not reduce lentiviral production nor infectivity, whereas the C fragment (MF
202 and ZnF) suppressed both lentiviral production and infectivity (Fig. 4b,c, Extended Data Fig. 3a). We
203 observed a similar tendency in the infectivity for other retroviruses (SIVmac, FIV, and EIAV)
204 (Extended Data Fig. 3b). Together, these results demonstrated that the C-terminal fragment of
205 ZCCHC3 had suppressive effect on HIV-1 and other retroviruses.
206 Because GagNC interacts with viral genomic RNA and promotes genome packaging into the virion[33],
207 we speculated that ZCCHC3 inhibits the interaction between GagNC and viral RNA (Fig. 4d).
208 Accordingly, we tested the effect of the C fragment of ZCCHC3 on RNA binding of GagNCp7 in an
209 RNA pull-down assay. The presence of the ZCCHC3 fragment abolished the binding (Fig. 4d). This
210 result strongly supported the notion that ZCCHC3 directly binds to GagNC. We further tested whether
211 the amount of incorporated viral RNA affected the viral production. It is established that each viral
212 particle contains a dimerized genomic RNA in its viral core, and the dimerized genomic RNA is critical
213 for interaction with GagNC[41]. To this end, we produced a lentiviral vector with different amounts of

214 transfer vector. We observed that increasing the amount of viral RNA augmented viral production
215 (Extended Data Fig. 3c). This observation supports our result that reduction of viral RNA by ZCCHC3
216 in producer cells leads to decreased virion production. Together, these results demonstrated that the C-
217 terminal fragment of ZCCHC3 inhibits the interaction between GagNC and viral RNA and reduces the
218 viral production.

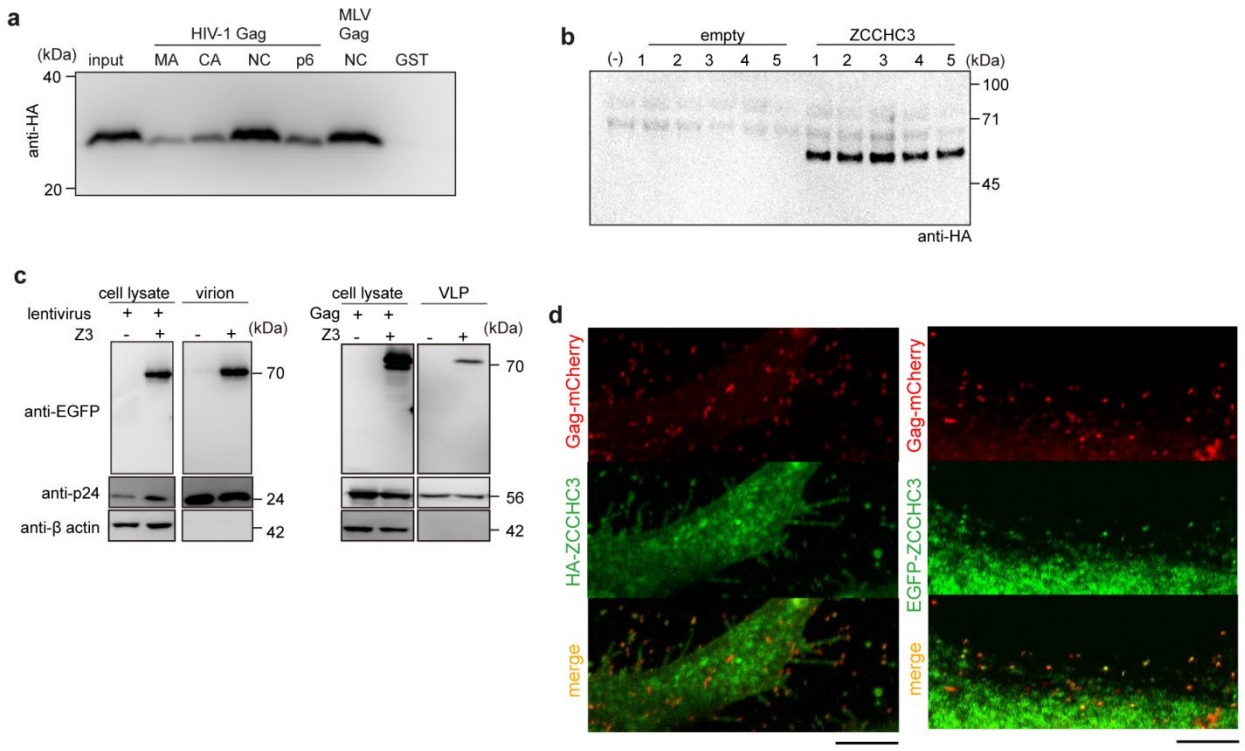

219

220 **Fig. 3| ZCCHC3 binding to GagNC. a**, ZCCHC3 binding to NCp7 of HIV-1 Gag. GST-tagged HIV-1 Gag MAp17,
221 CAp24, NCp7 or p6 protein, or MLV Gag NC was mixed with HEK293T cell lysate containing HA-ZCCHC3 and
222 GSH beads. The eluted fraction was analyzed by western blotting using an anti-HA antibody. A representative image
223 from three independent experiments is shown here. **b**, ZCCHC3 incorporated into the HIV-1 TF2625 virion. Lenti-
224 X 293T cells were transfected with pTF2625 plasmid in the presence or absence of a HA-ZCCHC3 expression
225 plasmid. Pelleted virions were analyzed by western blotting with a mouse anti-HA antibody (n = 5). **c**, Lentiviral
226 plasmids (pLV-EGFP, psPAX2, and pIIIenv3-1) (left) or a plasmid encoding HIV-1 Gag (right) were introduced into
227 HEK293T cells with or without a HA-ZCCHC3 expression plasmid. Virions were harvested by centrifugation, and
228 analyzed by immunoblotting with anti-EGFP, anti-p24, and anti-β-actin antibodies. **d**, Presence of ZCCHC3 in HIV-
229 1 Gag VLP. COS7 cells expressing HA-ZCCHC3 and mCherry-HIV-1 Gag were fixed, stained with an anti-HA
230 antibody, and observed using confocal laser scanning microscopy (CLSM) (left). COS7 cells expressing EGFP-
231 ZCCHC3 and mCherry-HIV-1 Gag were fixed and observed using CLSM (right). Scale bars, 5 μm.
232

233

234 ***ZCCHC3 interactions with GagNC***

235 The C-terminal fragment of ZCCHC3 contains three ZnF motifs. ZnFs are functionally versatile
236 structural motifs involved in various types of molecular interactions with DNA, RNA, and protein[42,43].
237 We therefore investigated the role of ZnFs in the antiviral effect of ZCCHC3. A pull-down assay using
238 purified GST-tagged GagNCp7 revealed that while the C fragment of ZCCHC3 strongly bound to
239 GagNCp7 (Fig. 4e), the deletion of ZnFs (the MF fragment) almost completely abolished the
240 interaction. This demonstrated that ZnFs are necessary for the interaction of ZCCHC3 and GagNCp7.
241 We then probed ZnF-mediated interaction with Gag in cultured cells. Specifically, mCherry-fused
242 GagNCp7 formed a liquid-like condensate in the cytoplasm (Fig. 4f, Extended Data Fig. 3d). Full-
243 length ZCCHC3 fused with EGFP, as well as EGFP-fused C fragment of ZCCHC3, colocalized with
244 the Gag condensate with a high partition coefficient (Fig. 4f,g). In good agreement with the pull-down
245 assay, the deletion of ZnFs (the MF fragment) severely abrogated the colocalization, and ZnF only
246 weakly associated with GagNCp7 (Fig. 4f,g). This demonstrated that while ZnF is necessary for the
247 interaction of ZCCHC3 with GagNC, the MF domain is also involved in the interaction. Notably, the
248 ZnF-mediated interaction with Gag was necessary for ZCCHC3 incorporation into the virion: the C
249 fragment, but not the MF fragment, was incorporated into Gag VLPs (Fig. 4h) and lentiviral virions
250 (Extended Data Fig. 3e). Together, these results indicated that ZnF is a primary site for ZCCHC3
251 interaction with GagNCp7, and plays a role in ZCCHC3 incorporation into the virion.

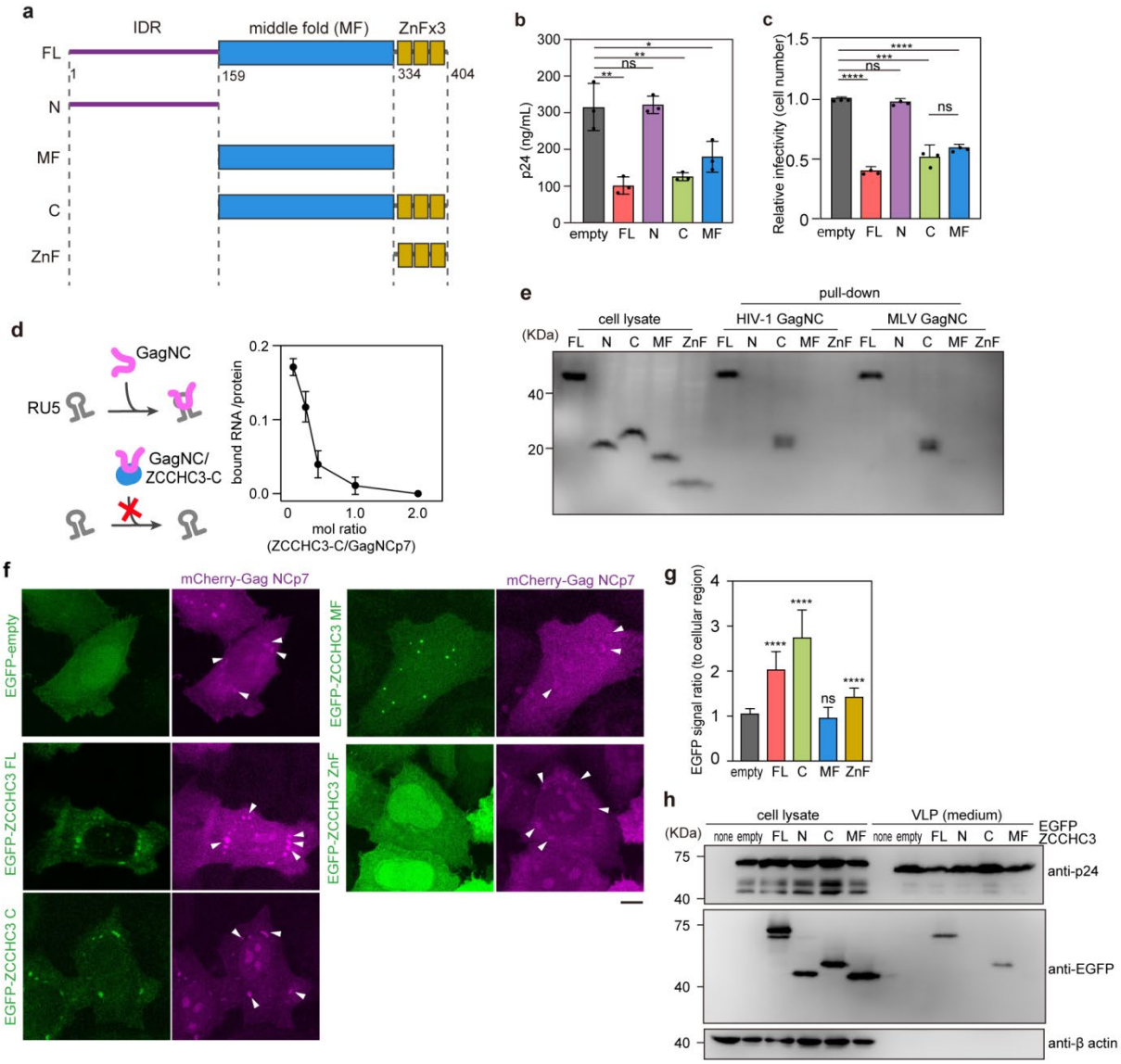

Fig. 4 ZCCHC3 binding to GagNC via C-terminal ZnFs. a, The domain structure of human ZCCHC3. IDR, MF, and zinc-finger (ZnF) domains are indicated. **b,c**, Effect of C-terminal fragment of ZCCHC3 on viral production and infectivity. HEK293T cells were transfected with lentiviral vectors, and a ZCCHC3 FL, N, C, or MF expression vector or an empty vector. The resultant lentiviruses were harvested 2 days after transfection and quantified by p24 ELISA (**b**). HeLa cells were infected with a p24-normalized amount of harvested lentiviruses, and infectivity quantified based on the expression of a viral gene (EGFP) using flow cytometry (**c**). The mean and standard deviation values from three independent experiments are shown. **d**, Hypothetical mechanism of ZCCHC3 inhibition of the interaction between Gag NC and viral RNA and the effect of ZCCHC3 on the interaction between HIV-1 Gag NCp7 and LTR RNA. Purified ZCCHC3 was tested in RNA pull-down assay of Gag NCp7 and HIV-1 LTR, at the molar ratios indicated. Fluorescent probe was used to quantify RNA (ng) in the bound fraction, which is presented as a ratio to the amount of the bait protein (ng) in the bound fraction quantified by Coomassie Brilliant Blue (CBB) staining. The mean and standard deviation values from three independent experiments are shown. **e**, Binding of different ZCCHC3 domains to Gag NCp7. GST-tagged HIV-1 or MLV Gag NC was mixed with HEK293T cell lysate containing HA-tagged ZCCHC3 FL, N, C, MF, or ZnF fragments, and the eluted fraction was analyzed by western blotting with anti-HA antibody. **f**,**g**, Localization of HIV-1 Gag NCp7 and ZCCHC3 in HeLa cells. HeLa cells

268 expressing mCherry-Gag NCp7 and EGFP-tagged ZCCHC3 FL, C, MF, or ZnF fragments were fixed and observed
269 using CLSM (**f**). The arrowheads indicate the cytoplasmic GagNC condensate. Scale bar, 5 μm. The fluorescence
270 intensity ratio of GagNC foci and cytoplasm was quantified (n = 15) (**g**). **h**, Incorporation of ZCCHC3 domains into
271 Gag VLP. Plasmid encoding EGFP-tagged ZCCHC3 FL, N, C, or MF was introduced into HEK293T cells together
272 with a plasmid encoding HIV-1 Gag. VLPs released into the culture medium were harvested and analyzed by
273 immunoblotting with anti-GFP, anti-p24, and anti-β-actin antibodies. **b**,**c**,**g**, Differences were examined by a two-
274 tailed, unpaired Student's *t*-test; ****$p < 0.0001$, ***$p < 0.001$, **$p < 0.01$, ns, $p \geq 0.05$.
275

276 ***ZCCHC3 interactions with retroviral RNA***

277 We next examined the role of MF domain in the antiviral effect of ZCCHC3. Although, based on pull-
278 down experiments with GST-tagged GagNCp7, the domain does not interact with Gag (Fig. 4e), it
279 nonetheless inhibited the infectivity of HIV-1, although the effect was approximately 10% weaker than
280 that of the C fragment (Fig. 4b,c). These observations suggested that the MF domain inhibits viral
281 production by a mechanism distinct from the ZnF-dependent interaction with Gag.
282 Accordingly, we next investigated the interaction between ZCCHC3 and viral RNA. According to a
283 structural prediction by AlphaFold2[44], the MF domain contains a basic cleft (Fig. 5a). Further, a
284 catRAPID prediction of RNA–protein interactions[45] identified several potential binding sites for HIV-
285 1 long terminal repeats (LTRs) within the MF domain (Extended Data Fig. 4a). Furthermore, our
286 previous experiments revealed that ZCCHC3 reduces the amount of Gag in Lenti-X-293T cells (Fig.
287 2a,b), although the amount of viral RNA was not affected by the presence of ZCCHC3 (Extended Data
288 Fig. 4b). Collectively, these observations suggested that ZCCHC3 functions at post-transcriptional
289 steps of viral production.
290 Accordingly, we investigated the interaction between the MF domain of ZCCHC3 and viral genome.
291 An RNA pull-down assay revealed that ZCCHC3 MF bound to R-U5 region of HIV-1 LTR and MLV
292 LTR, but not to the coding region of HIV-1 *gag* (Fig. 5b). The protein also bound to dsDNA and
293 ssDNA molecules carrying the same nucleotide sequences, but with a much lower affinity (Fig. 5b).
294 We obtained similar results in electrophoretic mobility shift assay (EMSA) (Fig. 5c). Unlike the
295 binding to GagNCp7, the MF domain was sufficient for binding to HIV-1 LTR (Fig. 5d) and to LTRs

296 of other retroviruses (Extended Data Fig. 4c).

297 The LTR of HIV-1 contains three stem-loop structures (Fig. 5e). To identify the region of HIV-1 LTR
298 that interacts with ZCCHC3 MF, we performed a RNA pull-down assay with the individual stem-loops,
299 which revealed that ZCCHC3 MF bound to all these structures (Fig. 5d). Further, screening of
300 ZCCHC3 MF variants with single substitutions of basic amino acid residues in the middle basic cleft
301 (Fig. 5a) identified two residues (R168 and R247) involved in RNA binding; a single substitution
302 (R168S and R247S) reduced the affinity for LTR RNA to approximately 50% of that of the wild type,
303 and the double substitution (R168/247S) further reduced to approximately 15% (Fig. 5f). Together,
304 these results demonstrated that ZCCHC3 binds to LTR RNA via its MF domain.

305

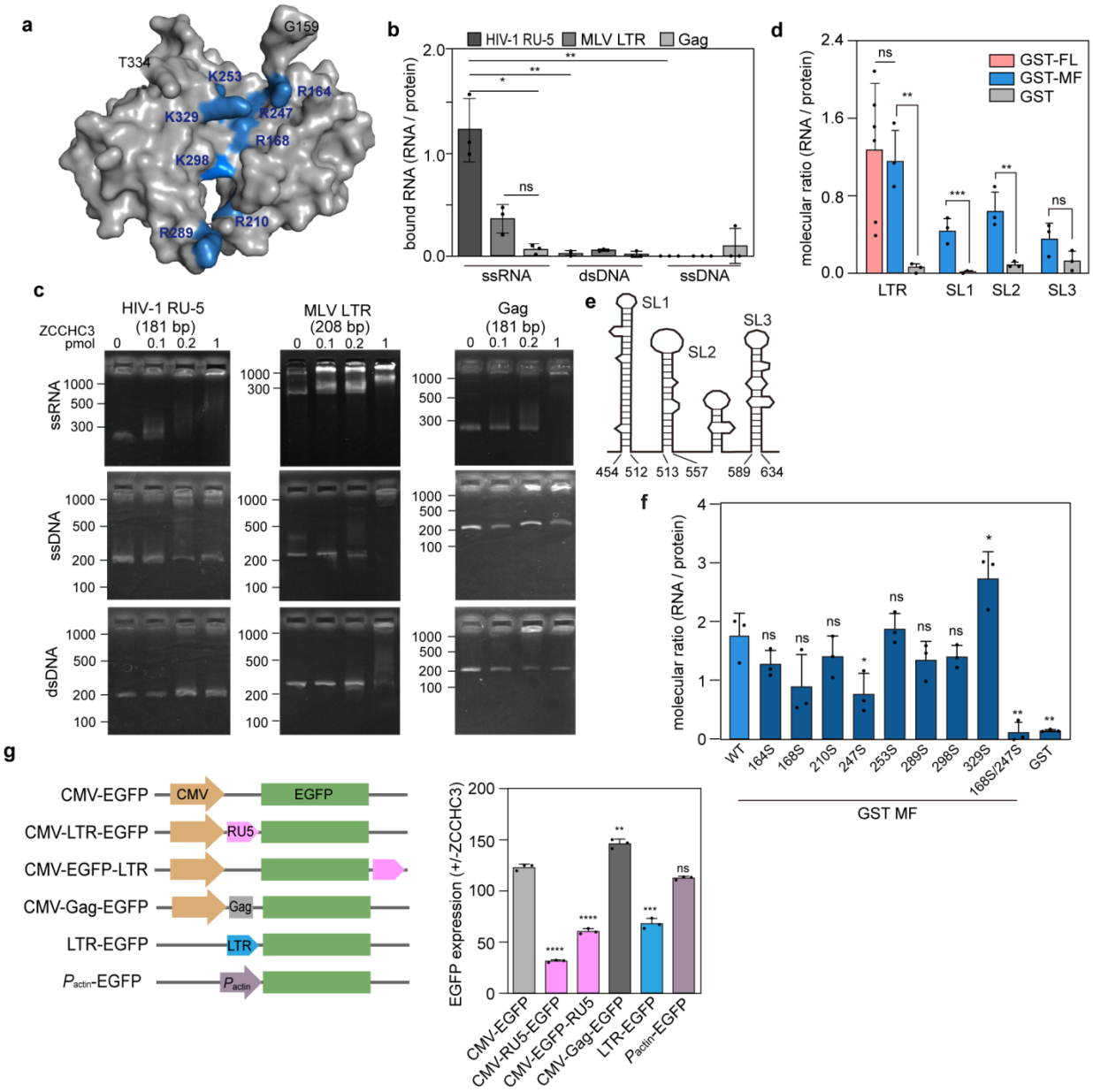

Fig. 5| ZCCHC3 binding to retroviral RNA. a, 3-D structure of ZCCHC3 MF region predicted by using AlphaFold2. Basic residues in the central cleft are labelled in blue. **b**, ZCCHC3 MF domain binding to LTR RNAs of HIV-1 and MLV. GST-tagged ZCCHC3 MF or GST was mixed with ssRNA, dsDNA, or ssDNA of HIV-1 LTR (R-U5), MLV LTR, or a coding region of Gag. Nucleic acids in the bound fraction were quantified using a fluorescent probe, and the amount is presented as a molecular ratio to the bait protein. The mean and standard deviation values from three independent experiments are shown. **c**, EMSA analysis of ZCCHC3–HIV-1 genome interaction. Different amounts of purified ZCCHC3 were incubated with ssRNA, dsDNA, and ssDNA (0.1 pmol, prepared as in **b**) and analyzed. **d**, Binding of ZCCHC3 domains to LTR. RNA pull-down assay was performed with HIV-1 LTR (R-U5) and GST-tagged ZCCHC3 FL or MF as described in (**b**). The amount of bound RNA is presented as the molecular ratio to the bait protein, with the mean and standard deviation values from three independent experiments shown. **e**, Schematic illustration of HIV-1 LTR (R-U5) secondary structure. **f**, Binding of ZCCHC3 MF domain to the stem-loops of HIV-1 LTR (R-U5). RNA pull down assay was performed with the SL1, SL2, or SL3 RNA, and GST-ZCCHC3 MF (WT or R168/247S), as described in (**d**). The amount of bound RNA is presented as the molecular ratio to the bait protein, with the mean and standard deviation values from three independent experiments shown. **g**,

Different EGFP-expressing constructs with the transcription of EGFP gene. HIV-1 LTR (R-U5) was inserted upstream or downstream of the *EGFP* ORF (left). A fragment of HIV-1 Gag gene (181 bp) was used as a control. Some constructs carry HIV-1 LTR (full length) or chicken β-actin promoter in place of the CMV promoter. The EGFP reporter constructs were introduced into HEK293T cells with or without a HA-ZCCHC3 expression plasmid, and EGFP fluorescence was quantified by flow cytometry. Quantification of EGFP-expressing cells as the ratio of signal between cells with (+) and without (–) HA- ZCCHC3 is shown (right). The mean and standard deviation values from three independent experiments are shown. Differences in **d** and **f** were examined by a two-tailed, unpaired Student's *t*-test. ***$p < 0.001$, **$p < 0.01$, *$p < 0.05$; ns, $p \geq 0.05$. Differences in **g** were examined by a two-tailed, unpaired Student's *t*-test, followed by Welch's correction. ****$p < 0.0001$, ***$p < 0.001$, ** $p < 0.005$; ns, $p \geq 0.01$.

ZCCHC3 and viral RNA in P-body

Previously, proteomic analysis identified ZCCHC3 in the P-body, a membrane-less organelle that sequesters various mRNAs and inhibits protein production[46]. We therefore speculated that ZCCHC3 delivers viral RNA to the P-body and thus suppresses viral protein production. Indeed, immuno-staining of HEK293T cells with ZCCHC3 and a P-body marker protein (LSM14a) revealed that endogenous ZCCHC3 was present in the P-bodies (Fig. 6a). Overexpression of ZCCHC3 increased both, the number of P-bodies in a cell and the colocalization of ZCCHC3 in P-bodies (Fig. 6a). To confirm the interaction between ZCCHC3 and the P-body, we performed proximity-dependent biotin identification of proteins (BioID analysis) using TurboID-fused ZCCHC3. We identified 610 proteins (1,228 biotinylated peptides) as spatial neighbours of ZCCHC3, including some P-body proteins (Fig. 6b). Enrichment analysis using GO terms revealed a nearly 100-fold enrichment of P-body proteins among the biotinylated proteins (Fig. 6c). Notably, lentiviral infection and the expression of LTR-carrying RNA increased the number of P-bodies and localization of ZCCHC3 in the P-bodies (Fig. 6a,d,e). Further, the MF domain, which binds to LTR RNA, was necessary and sufficient for P-body localization of ZCCHC3 (Fig. 6f). Collectively, these results suggested that ZCCHC3 recognizes LTR-carrying RNA and sequesters it to the P-body.

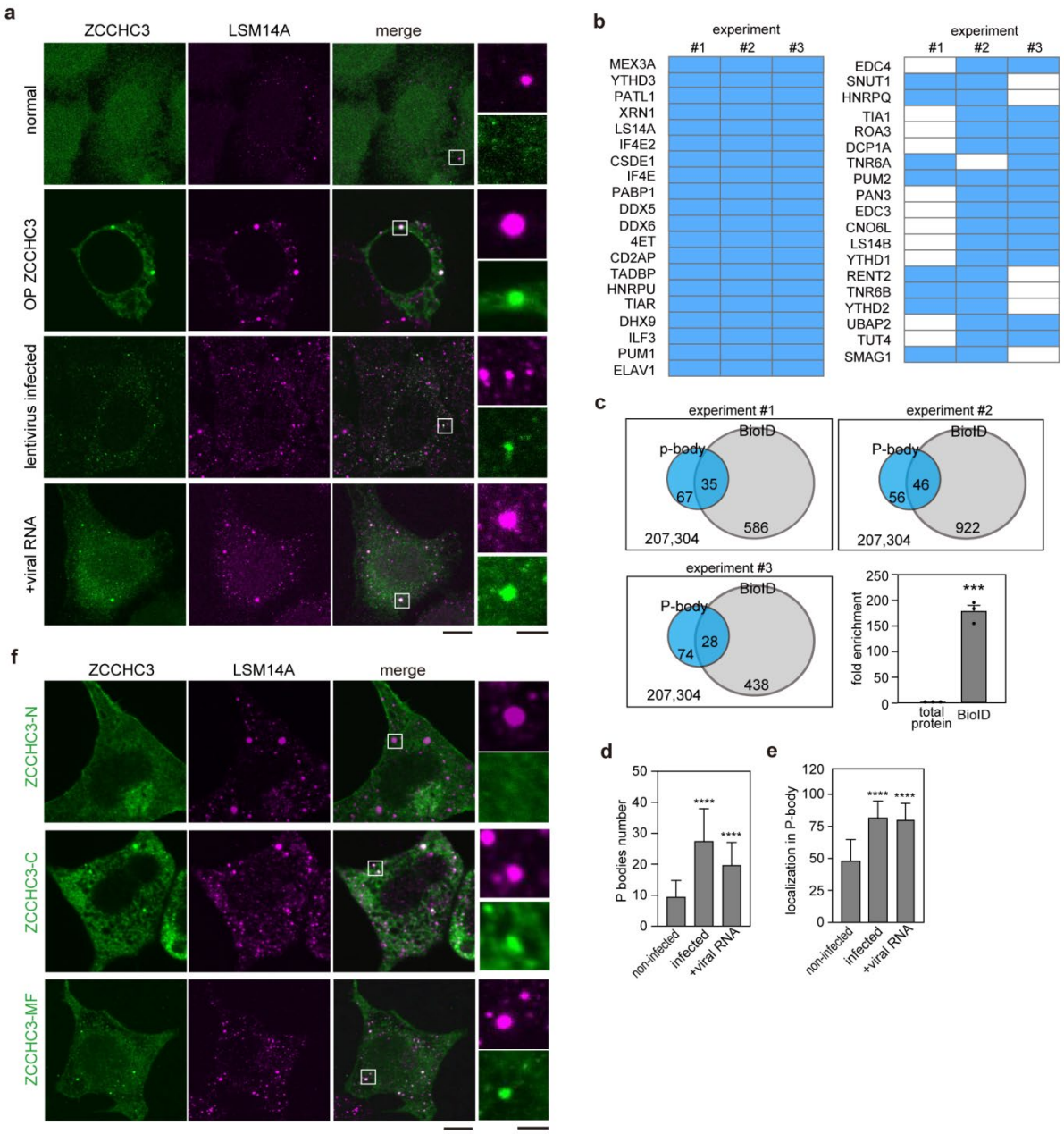

Fig. 6| ZCCHC3 sequestration of viral RNA in P-body. a,**d**,**e**, ZCCHC3 localization in the P-body. 293T cells were infected with lentivirus, or transfected with a plasmid encoding EGFP-ZCCHC3 or HIV-1 LTR, and immuno-stained with anti-LSM14A and anti-ZCCHC3 antibodies. Representative images are shown (**a**). Scale bar, 5 µm. The numbers of LSM14A-positive foci per cell are shown in (**d**), with 20 cells analyzed per group. Colocalization of ZCCHC3 and LSM14A was also quantified (**e**). Differences were examined by a two-tailed, unpaired Student's *t*-test. ****$p < 0.0001$. **b**,**c**, BioID analysis of 293T cells stably expressing TurboID-fused ZCCHC3. P-body proteins were extracted from the set of identified proteins using GO terms and are shown for three independent experiments (**b**). The original data of mass spectrometry is provided in Supplementary Table 2. The total number of proteins identified in individual experiments are summarized in a Venn diagram (**c**). Fold enrichment of P-body proteins is shown as the mean and standard deviation (n = 3; **c**, right bottom panel). Differences were examined by a two-tailed, unpaired Student's *t*-test. ***$p < 0.001$. **f**, The role of ZCCHC3 MF domain in P-body localization. HEK293T cells expressing EGFP-tagged fragments (N, MF, C) of ZCCHC3 were immuno-stained with an anti-LSM14A antibody and observed using CLSM. Scale bars, 5 µm (left panels), 1µm (right panels).

361 **Discussion**

362 In the current study, we demonstrated that ZCCHC3 is a novel HIV-1 restriction host factor, which
363 acts on multiple viral components (GagNC and LTR) to suppress viral production and infectivity. We
364 showed that ZCCHC3 binds to GagNC primarily via ZnFs and prevents it from binding to viral RNA.
365 This results in the assembly of ZCCHC3-loaded virions, not genome-loaded virions (Extended Data
366 Fig. 5). Further, ZCCHC3 binds to the LTR of viral genomic RNA via the basic pocket in the MF
367 domain and sequesters the viral genomic RNA in the P-body (Extended Data Fig. 5). Notably,
368 ZCCHC3 also suppresses a wide spectrum of retroviruses and is not antagonized by viral proteins.
369 These unique properties make ZCCHC3 distinct from other known restriction factors.

370 ZCCHC3 and APOBEC3G, a well-researched HIV-1 restriction factor antagonized by viral Vif protein,
371 are similar in that both can interact with HIV-1 genomic RNA[47] and are incorporated in the HIV-1
372 virion in a GagNC-dependent manner[48]. However, the antiviral mechanism of ZCCHC3 is clearly
373 distinct from that of APOBEC3G: ZCCHC3 sequesters the viral RNA in the P-body (Fig. 6a,b),
374 whereas APOBEC3G increases the mutation rate at the reverse transcription step of viral life cycle[46].
375 Although APOBEC3G was detected in the P-body[49], the functional significance of this observation for
376 the antiviral effect of this protein is not known. In addition, unlike ZCCHC3 (Fig. 1c,d), APOBEC3G
377 and other known host restriction factors are antagonized by HIV-1 accessory proteins (i.e., Vif, Vpr,
378 Vpu, and Nef) and capsid mutations[50–52].

379 We found that the ZCCHC3–viral RNA interaction is mediated by the MF domain (a.a. 159–334) but
380 not the ZnF domain (a.a. 334–404) (Fig. 5d). The ZnF domain plays a major role in the protein's
381 interaction with GagNC (Fig. 4e,f,g). That was unexpected because in many host restriction factors,
382 ZnF motifs are mainly involved in viral RNA binding[53]. Previously, ZCCHC3 ZnF was shown to bind
383 to dsRNA and poly I:C with a K_d of 40 nM, although the protein fragment assayed in the previous
384 study (a.a. 300–404) also contained a part of the MF domain[30]. Mutagenesis experiments presented
385 herein revealed that two basic residues of ZCCHC3, R168 and R247, are involved in viral RNA

386 binding. These two residues are predicted to be located opposite one another within the middle cleft
387 (Fig. 5a). The predicted 3D structure of this RNA binding motif is distinct from that of any other
388 known RNA-binding motifs. Crystal structures of ZCCHC3 MF fragment and its complex with viral
389 RNA are needed to confirm the spatial relationship between the two identified residues, and their roles
390 in interactions with viral RNA.

391 The interaction between ZCCHC3 (ZnFs) and GagNC is a novel type of protein–protein interaction.
392 Both proteins contain CCHC-type ZnFs (3 and 2, accordingly). We observed that mCherry-fused
393 GagNCp7 formed a liquid-like condensate in the cytoplasm when it was overexpressed in HEK293T
394 cells (Fig. 4f, Extended Data Fig. 3d). This is in good agreement with a recent study demonstrating
395 that GagNC undergoes liquid–liquid phase separation (LLPS) together with viral RNA, which plays a
396 critical role in viral packaging and maturation[54]. We found that ZCCHC3 colocalized in GagNC
397 condensate in a ZnF-dependent manner (Fig. 4f,g). This result implies that CCHC ZnFs undergo LLPS
398 in the intracellular milieu, and that ZCCHC3 utilizes this mechanism to associate with the viral
399 component. Indeed, recent studies demonstrated that CCHC-type ZnF, as well as other types of ZnF,
400 undergo LLPS, both *in vivo* and *in vitro*[55,56]. While Zn^{2+}-mediated conformation of the CCHC
401 sequence and/or electrostatic interactions among charged residues within and between individual ZnFs
402 could be involved in the ZCCHC3–GagNC interaction, further structural and functional studies are
403 required to elucidate the molecular details.

404 A limitation of this study is that most of the experiments herein used an overexpression system to test
405 the antiviral activity of ZCCHC3. To better understand the impact of the physiological level of
406 ZCCHC3 on HIV-1 replication, it will be interesting to use primary CD4+ T cells or macrophages for
407 the analysis. Our data showed that the ZCCHC3-containing virus showed significantly lower
408 infectivity in monocyte-derived THP-1 cells, suggesting that cell type may affect the antiviral activity
409 of ZCCHC3. Furthermore, the impact of the single nucleotide polymorphism (SNP) in the *Zcchc3* gene
410 on the anti-HIV-1 activity should be investigated. Overall, here, we demonstrated that ZCCHC3 is a

411 novel anti-HIV-1 host factor that evades antagonization by viral proteins. Given that ZCCHC3 targets
412 multiple steps of HIV-1 replication, it is important to test the therapeutic effect of its overexpression
413 in cells persistently or latently infected with HIV-1. Furthermore, structural and biochemical
414 investigations are required to design a modified ZCCHC3 with higher potency.
415

416 **References**

417 [1] Fauci, A.S. Host factors and the pathogenesis of HIV-induced disease. *Nature* **384**, 529–534 (1996).

418 [2] Ishii, K., et al. A Toll-like receptor–independent antiviral response induced by double-stranded B-
419 form DNA. *Nat Immunol.* **7**, 40–48 (2006).

420 [3] Ghimire, D., Rai, M. & Gaur, R. Novel host restriction factors implicated in HIV-1 replication. *J.*
421 *Gen Virol.* **99**, 435–446 (2018).

422 [4] Smith, H.C., Bennett, R.P., Kizilyer, A., William, M.M. & Kimberly, M.P. Functions and
423 regulation of the APOBEC family of proteins. *Semin Cell Dev Biol.* **23**, 258–268 (2012).

424 [5] Albin, J., & Harris, R. Interactions of host APOBEC3 restriction factors with HIV-1 in vivo:
425 Implications for therapeutics. *Expert Rev Mol Med.* **12**, e4 (2010).

426 [6] Sheehy, A.M., Gaddis, N.C. & Choi, J.D. Isolation of a human gene that inhibits HIV-1 infection
427 and is suppressed by the viral Vif protein. *Nature* **418**, 646–650 (2002).

428 [7] Yang, H., Kim, K., Li, S., Pacheco, J. & Chen, X. S. Structural basis of sequence-specific RNA
429 recognition by the antiviral factor APOBEC3G. *Nat Commun.* **13,** 1–15 (2022).

430 [8] Miyagi, E., et al. Enzymatically active APOBEC3G is required for efficient inhibition of human
431 immunodeficiency virus type 1. *J. Virol.* **81**, 13346–13353 (2007).

432 [9] Svarovskaia, E.S., et al. Human apolipoprotein B mRNA editing enzyme-catalytic polypeptide-
433 like 3G (APOBEC3G) is incorporated into HIV-1 virions through interactions with viral and
434 nonviral RNAs. *J. Biol. Chem.* **279**, 35822–35828 (2004).

435 [10] Hayakawa, S., et al. ZAPS is a potent stimulator of signaling mediated by the RNA helicase RIG-
436 I during antiviral responses. *Nat Immunol.* **12**, 37–44 (2011).

437 [11] Gao, G., Guo, X. & Goff, S.P. Inhibition of retroviral RNA production by ZAP, a CCCH-type
438 zinc finger protein. *Science* **297**, 1703–1706 (2022).

439 [12] Kerns, J.A., Emerman, M. & Malik, H.S. Positive selection and increased antiviral activity
440 associated with the PARP-containing isoform of human zinc-finger antiviral protein. *PLoS*

441 *Genet.* **4**, e21 (2008).

442 [13] Zhu, Y., et al. Zinc-finger antiviral protein inhibits HIV-1 infection by selectively targeting
443 multiply spliced viral mRNAs for degradation. *Proc Natl Acad Sci U S A.* **108**, 15834–15839
444 (2011).

445 [14] Contreras, X., et al. Nuclear RNA surveillance complexes silence HIV-1 transcription. *PLoS*
446 *Pathog.* **14**, e1006950 (2018).

447 [15] Goujon, C., et al. Human MX2 is an interferon-induced post-entry inhibitor of HIV-1 infection.
448 *Nature* **502**, 559–562 (2013).

449 [16] Sokolskaja, E., Berthoux, L. & Luban, J. Cyclophilin A and TRIM5α independently regulate
450 human immunodeficiency virus type 1 infectivity in human cells. *J. Virol.* **80**, 2855–2862 (2006).

451 [17] O'Connor, C., et al. p62/sequestosome-1 associates with and sustains the expression of retroviral
452 restriction factor TRIM5α. *J. Virol.* **84**, 5997–6006 (2010).

453 [18] Neil, S. J.D., Zang, T. & Bieniasz, P.D. Tetherin inhibits retrovirus release and is antagonized by
454 HIV-1 Vpu. *Nature* **451**, 425–430 (2008).

455 [19] Perez-Caballero, D., et al. Tetherin inhibits HIV-1 release by directly tethering virions to cells.
456 *Cell* **139**, 499–511 (2009).

457 [20] Hrecka, K., et al. Vpx relieves inhibition of HIV-1 infection of macrophages mediated by the
458 SAMHD1 protein. *Nature* **474**, 658–661 (2011).

459 [21] Laguette, N., et al. SAMHD1 is the dendritic-and myeloid-cell-specific HIV-1 restriction factor
460 counteracted by Vpx. *Nature* **474**, 654–657 (2011).

461 [22] Compton, A.A., et al. IFITM proteins incorporated into HIV-1 virions impair viral fusion and
462 spread. *Cell Host Microbe* **16,** 736–747 (2014).

463 [23] Saitoh, T., et al. Antiviral protein Viperin promotes Toll-like receptor 7-and Toll-like receptor 9-
464 mediated type I interferon production in plasmacytoid dendritic cells. *Immunity* **34**, 352–363
465 (2011).

466 [24] Medzhitov, R. & Janeway, Jr. C. Innate immune recognition: mechanisms and pathways. *Immunol*
467 *Rev.* **173**, 89–97 (2000).
468 [25] Sun L., et al. Cyclic GMP-AMP synthase is a cytosolic DNA sensor that activates the type I
469 interferon pathway. *Science* **339**, 786–791 (2013).
470 [26] Engeland, C.E., et al. Proteome analysis of the HIV-1 Gag interactome. *Virology* **460**, 194–206
471 (2014).
472 [27] Chen, X., et al. Proteomic analysis reveals zinc-finger CCHC-type containing protein 3 as a factor
473 inhibiting virus infection by promoting innate signalling. *Virus Res.* **319**, 198876 (2022).
474 [28] Lian, H., et al. ZCCHC3 is a co-sensor of cGAS for dsDNA recognition in innate immune
475 response. *Nat Commun.* **9**, 3349 (2018).
476 [29] Lian H., et al. The zinc-finger protein ZCCHC3 binds RNA and facilitates viral RNA sensing and
477 activation of the RIG-I-like receptors. *Immunity* **49**, 438–448. e5 (2018).
478 [30] Kang DC., et al. mda-5: An interferon-inducible putative RNA helicase with double-stranded
479 RNA-dependent ATPase activity and melanoma growth-suppressive properties. *Proc Natl Acad*
480 *Sci U S A.* **99**, 637–642 (2002).
481 [31] Chen, X., et al. Host Zinc-finger CCHC-type containing protein 3 inhibits pseudorabies virus
482 proliferation by regulating type I interferon signalling. *Gene* **827**, 146480 (2022).
483 [32] Derdeyn, C.A., et al. Sensitivity of human immunodeficiency virus type 1 to the Fusion Inhibitor
484 T-20 is modulated by coreceptor specificity defined by the V3 loop of gp120. *J Virol.* **74** , 8358–
485 8367 (2022).
486 [33] Platt, E.J., Wehrly, K., Kuhmann, S.E., Chesebro, B. & Kabat, D. Effects of CCR5 and CD4 Cell
487 Surface Concentrations on Infections by Macrophagetropic Isolates of Human
488 Immunodeficiency Virus Type 1. *J Virol.* **72**, 2855–2864 (1998).
489 [34] Platt, E.J., Bilska, M., Kozak, S.L., Kabat, D. & Montefiori, D.C. Evidence that ecotropic murine
490 leukemia virus contamination in TZM-bl cells does not affect the outcome of neutralizing

491 antibody assays with human immunodeficiency virus type 1. *J Virol.* **83**, 8289–8292 (2009).

492 [35] Takeuchi, Y., McClure, M.O. & Pizzato, M. Identification of gammaretroviruses constitutively
493 released from cell lines used for human immunodeficiency virus research. *J Virol.* **82**, 12585–
494 12588 (2008)

495 [36] Wei, X., et al. Emergence of resistant human immunodeficiency virus type 1 in patients receiving
496 fusion inhibitor (T-20) monotherapy. *Antimicrob Agents Chemother.* **46**, 1896–1905 (2002).

497 [37] Wang, S., et al. Modification of N-terminal a-amine of proteins via biomimetic ortho-quinone-
498 mediated oxidation. *Nat Commun.* **12**, 2257 (2021).

499 [38] Sun, X., Yau, V. K., Briggs, B. J., et al. Role of clathrin-mediated endocytosis during vesicular
500 stomatitis virus entry into host cells. *Virology* **338**, 53–60 (2005).

501 [39] Lee, K.E., et al. Flexible use of nuclear import pathways by HIV-1. *Cell Host Microbe* **7**, 221–
502 233 (2010).

503 [40] Sultana, T., et al. Novel mutant human immunodeficiency virus type 1 strains with high degree
504 of resistance to cynomolgus macaque TRIMCyp generated by random mutagenesis. *J Gen Virol.*
505 **97**, 963–976 (2016).

506 [41] Lu, K., Heng, X., Garyu, L., et al. NMR detection of structures in the HIV-1 5′-leader RNA that
507 regulate genome packaging. *Science*, **334**, 242-245 (2011).

508 [43] Gamsjaeger, R., et al. Sticky fingers: zinc-fingers as protein-recognition motifs. *Trends Biochem*
509 *Sci.* **32**, 63–70 (2007).

510 [44] Kluska, K., Adamczyk, J. & Krężel, A. Metal binding properties, stability and reactivity of zinc
511 fingers. *Coord Chem Rev*. **367**, 18–64 (2018).

512 [44] Jumper, J., et al. Highly accurate protein structure prediction with AlphaFold. *Nature* **596**, 538-
513 589 (2021) .

514 [45] Agostini, F., et al. cat RAPID omics: a web server for large-scale prediction of protein–RNA
515 interactions. *Bioinformatics* **29**, 2928–2930 (2013).

516 [46] Luo, Y., Na, Z. & Slavoff, S.A. P-bodies: composition, properties, and functions. *Biochemistry*
517 **57**, 2424–2431 (2018).
518 [47] Liddament, M.T., Brown, W.L., Schumacher, A.J. & Harris, R.S. APOBEC3F properties and
519 hypermutation preferences indicate activity against HIV-1 in vivo. *Curr Biol.* **14**, 1385–1391
520 (2004).
521 [48] Cen, S., et al. The interaction between HIV-1 Gag and APOBEC3G. *J Bio Chem.* **279**, 33177–
522 33184 (2004).
523 [49] Phalora, P.K., Sherer, N.M., Wolinsky, S.M., Swanson, C.M. & Malim, M.H. HIV-1 replication
524 and APOBEC3 antiviral activity are not regulated by P bodies. *J Virol.* **86**, 11712–11724 (2012).
525 [50] Daniel, S. & Frank, K. Key viral adaptations preceding the AIDS pandemic. *Cell Host Microbe*
526 **25**, 27–38 (2019).
527 [51] Ito, F., et al. Structural basis for HIV-1 antagonism of host APOBEC3G via Cullin E3 ligase. *Sci*
528 *Adv.* **9**, eade3168 (2023).
529 [52] Sowd, G.A., Shi, J. & Aiken, C. HIV-1 CA inhibitors are antagonized by inositol phosphate
530 stabilization of the viral capsid in cells. *J Virol.* **95**, e01445–e01421 (2021).
531 [53] Corley, M., Burns, M.C. & Yeo, G.W. How RNA-binding proteins interact with RNA: molecules
532 and mechanisms. *Mol Cell.* **78**, 9–29 (2020).
533 [54] Monette, A., et al. Pan-retroviral nucleocapsid-mediated phase separation regulates genomic RNA
534 positioning and trafficking. *Cell Rep.* **31**, 07520 (2020).
535 [55] Wang, Y., et al. The distinct roles of zinc finger CCHC-type (ZCCHC) superfamily proteins in
536 the regulation of RNA metabolism. *RNA Bio.* **18**, 2107–2126 (2021).
537 [56] Du, M., Ea, C.K., Fang, Y. & Chen, Z.J. Liquid phase separation of NEMO induced by
538 polyubiquitin chains activates NF-κB. *Mol Cell.* **82**, 2415–2426. e5 (2022).
539
540

541 **Methods**

542 ***Materials***

543 The following reagents were obtained through the NIH HIV Reagent Program, Division of AIDS,
544 NIAID, NIH: HIV-1, Strain NL4-3 Infectious Molecular Clone (pNL4-3) (ARP-2852[57]) contributed
545 by Dr. M. Martin, Panel of Full-Length Transmitted/Founder (T/F) HIV-1 Infectious Molecular Clones
546 (ARP-11919[58,59]) contributed by Dr. John C. Kappes, Human Immunodeficiency Virus Type 2 (HIV-
547 2) ST Infectious Molecular Clone (ARP-12444) contributed by Dr. Beatrice Hahn and Dr. George
548 Shaw, SIVcpzTAN 2.69 Infectious Molecular Clone (ARP-11497[60]) and SIVcpzTAN3.1 Infectious
549 Molecular Clone (ARP-11498[60]) contributed by Drs. Jun Takehisa, Matthias H. Kraus and Beatrice H.
550 Hahn, SIVagmSab92018ivTF (ARP-12140) contributed by Drs. Frank Kirchhoff, Clement
551 Gnanadurai, and Beatrice Hahn, and SIV Packaging Construct (SIV3+, ARP-13456) and SIV LTR
552 Luciferase mCherry Reporter Vector (ARP-13455) contributed by Dr. Tom Hope. psPAX2-IN/HiBiT
553 and pWPI-Luc2 were kind gifts from Dr. Kenzo Tokunaga[61]. pMSMnG was a kind gift from Dr. Jun-
554 ichi Sakuragi[62]. pLionII (1730; http://n2t.net/addgene:1730; RRID: Addgene_1730) and pCPRDEnv
555 (1732; http://n2t.net/addgene:1732; RRID: Addgene_1732) were gifts from Dr. Garry Nolan. pEIAV-
556 SIN6.1 CGFPW (44171; http://n2t.net/addgene:44171; RRID: Addgene_44171) and pEV53D (44168;
557 http://n2t.net/addgene:44168; RRID: Addgene_44168) were gifts from Dr. John Olsen. lentiCRISPR
558 v2 was a gift from Feng Zhang (Addgene plasmid# 52961; http://n2t.net/addgene:52961; RRID:
559 Addgene_52961)[63]. pMD2.G (12259; http://n2t.net/addgene:12259; RRID: Addgene_12259) and
560 psPAX2 (12260; http://n2t.net/addgene:12260; RRID: Addgene_12260) were gifts from Dr. Didier
561 Trono. pLV-eGFP was a gift from Dr. Pantelis Tsoulfas (36083; http://n2t.net/addgene:36 083; RRID:
562 Addgene_36083)[64]. pGP (# 6161) and pDON-5 Neo DNA (# 3657) were purchased from Takara Bio
563 Inc. (Shiga, Japan). The luciferase-encoding and ZsGreen-encoding retroviral vectors were described
564 previously[64].

565

566 ***DNA constructions***

567 The cDNA encoding human ZCCHC3 (NM_033089.7) was amplified from cDNA pool of HeLa cells
568 by PCR and cloned into pEGFP-C3 (Takara Bio Inc., Shiga, Japan), pCMV-HA-N2 (Takara Bio Inc.,),
569 pET28a(+) (Takara Bio Inc.) or pGEX6P1 (Cytiva, Marlborough, MA, USA). Fragments of the
570 ZCCHC3 N-terminus (a.a. 1 - 159), ZCCHC3 C terminus (a.a. 159- 404), ZCCHC3 MF fragment (a.a.
571 159- 334) and ZCCHC3 ZnF fragment (a.a. 334- 404) were amplified by PCR using KOD-Plus-Neo
572 (# KOD-401, TOYOBO, CO., ltd., Osaka, Japan), and subcloned into pEGFP-C3 and pCMV-HA-N2
573 for mammalian expression. Fragments of ZCCHC3 C terminus (a.a. 159- 404) and ZCCHC3 MF
574 fragment (a.a. 159- 334) were amplified by PCR and subcloned into pET28a(+), for ZCCHC3 MF
575 fragment also pGEX6P1 for expression in *Escherichia coli*. The cDNA encoding human cGAS
576 (NM_138441.3) was purchased from Addgene (#108674) and subcloned into pEGFP-C3 vector.

577 The ZCCHC3 MF fragments carrying amino acid substitution(s) were generated by replacing the
578 amino acids of R164, R168, R210, R247, K253, R289, K298 or K329 with S, respectively; the
579 R268SR247S mutation was generated by replacing the amino acid of R168 and R247 with S. Single,
580 and double amino acid mutations were introduced using PrimerSTAR® Max DNA Polymerase (#
581 R046A, Takara Bio Inc.). The primers used for the mutation generation were listed in SI data.

582 The whole Gag sequence was amplified from wild-type Gag plasmid by PCR and cloned into
583 pGEX6P1 and pmCherry-C1 (Takara Bio Inc.). Fragments of MAp17 (a.a. 1 - 132), CAp24 (a.a. 133
584 - 363), Gag NCp7 (a.a. 378 - 432) and p6 (a.a. 449 - 500) were amplified by PCR using KOD-Plus-
585 Neo and subcloned into pGEX6P1 for expression in *Escherichia coli*.

586 The DNA fragments encoding 5'-LTR (454 - 634 nt, GenBank: MN989412.1) and Gag protein (1-181
587 nt) of HIV-1 were amplified by PCR using KOD-Plus-Neo and pNL4-3 as a template and cloned into
588 pBluescript II KS(-) (212208, Agilent). The MLV 5'-LTR (1 - 207 nt, GenBank: KU324804.1)
589 sequence was amplified from pDON-5 Neo, the EIAV 5′ LTR (1 - 114 nt, GenBank: AF247394.1)
590 was amplified from pEIAV-SIN6.1 CGFPW, and SIV 5′ LTR (1 - 351 nt, GenBank: DQ374657.1)

591 was amplified from SIVcpzTAN 2.69 and cloned into pBluescript II KS(-).

592 To generate reporter constructs, HIV-1 5'-LTR (FL) (377 - 634 nt, GenBank: MN989412.1), HIV-1
593 5'-LTR (R-U5) region (377 - 634 nt, GenBank: MN989412.1), a coding region of *gag* (3023 - 3203
594 nt, GenBank: MN989412.1), β-actin promoter on pCAGGS (386 - 661 nt) were amplified by PCR
595 using KOD-Plus-Neo. The R-U5 fragment was cloned into NheI/AgeI or XhoI/EcoRI sites of pEGFP-
596 C1 to generate CMV-LTR-EGFP or CMV-EGFP-LTR, respectively. The gag fragment was cloned
597 into NheI/AgeI sites of pEGFP-C1 to generate CMV-gag-EGFP. The LTR (FL) fragment or the β-
598 actin promoter fragment was cloned into AseI/NheI sites of pEGFP-C1 to generate LTR-EGFP or
599 Pactin-EGFP, respectively. Information of all the primers and restriction sites for cloning is
600 summarized in Supplementary Table 1.

601

602 ***Cell culture***

603 TZM-bl cells (ARP-8129[32-37]) were obtained through the NIH HIV Reagent Program, Division of
604 AIDS, NIAID, NIH (contributed by Dr. John C. Kappes, Dr. Xiaoyun Wu and Tranzyme Inc.) Lenti-
605 X 293T cells (Takara Bio Inc.), TZM-bl cells, HEK293T and COS7 cells (0539, Riken BRC Cell
606 Bank) were cultured in Dulbecco's Modified Eagle Medium (DMEM) high glucose (08468-16, Nacalai
607 Tesque, Kyoto, Japan), while HeLa S3 cells (ATCC, CCL-2.2,) were cultured in DMEM with low
608 glucose (D6046, Sigma-Aldrich, St. Louis, MO, USA), supplied with 10% (v/v) fetal bovine serum
609 (FBS) (173012, Sigma-Aldrich). HeLa CD4 cells (NIH AIDS reagent program) were maintained in
610 DMEM supplemented with 10% (v/v) FBS and 2 mg/mL G418 (16512-81, Nacalai Tesque, Kyoto,
611 Japan). MT4 cells ((JCRB1216, Japanese Collection of Research Bioresources Cell Bank)), C8166-
612 CCR5 cells, and THP-1 cells were cultured in RPMI-1640 (R8758, Sigma-Aldrich) supplemented with
613 10% (v/v) FBS. For passaging the adherent cells, cells were treated with 2.5 g/L- trypsin/EDTA
614 solution (32777-44, Nacalai Tesque). All the cells were incubated in a humidified incubator at 37 °C
615 with 5 % CO_2.

616

617 ***Plasmid transfection, virus production and collection, virus infection***

618 Plasmid DNAs were introduced into Lenti-X 293T or HEK293T cells using either polyethylenimine
619 hydrochloride (PEI) (49553-93-7, Polyscience, Niles, IL, USA) or TransIT®-293 Transfection Reagent
620 (MIR2700, Mirus Bio LLC, Madison, WI, USA). For production of VSV-G-pseudotyped HIV-1,
621 Lenti-X 293T cells were co-transfected with pMSMnG and pMD2.G plasmids. The supernatant was
622 collected and filtered 48 h after transfection. For production of lentivirus, a transfer vector (pLV-EGFP
623 or pWPI-Luc2) was introduced into HEK293T or Lenti-X 293T cells together with a packaging vector
624 (psPAX2 or psPAX2-IN/HiBiT) and an envelope vector (pMD2.G) at a ratio of 5:3:2. The culture
625 medium was collected 48 h after the transfection and centrifuged at 1,500 g for 10 min at 4 °C to
626 remove cell debris. For other plasmid transfections, PEI was used.

627 Both lentiviral and retroviral vectors were rescued as described previously in the presence or absence
628 of pCMV-HA-ZCCHC3 plasmids[65]. To rescue an SIVmac-based lentiviral vector, Lenti-X 293T cells
629 were co-transfected with the pSIV3+ plasmid, SIV LTR Luciferase mCherry Reporter Vector, and
630 pMD2.G plasmid. To rescue an FIV-based lentiviral vector, Lenti-X 293T cells were co-transfected
631 with the pCPRDEnv, pLionII-luc2, and pMD2.G plasmids. To rescue an EIAV-based lentiviral vector,
632 Lenti-X 293T cells were co-transfected with pEV53D, EIAV-SIN6.1-luc2, and pMD2.G plasmids. To
633 rescue an MLV-based retroviral vector, Lenti-X 293T cells were co-transfected with pGP, pDON-5
634 Neo-luc2, and pMD2.G plasmids. The supernatant was collected and filtered 48 h after transfection.

635 Expression and processing of Gag proteins in Lenti-X 293T cells were evaluated with western
636 blot. Lenti-X 293T cells transfected with either TF2625, pNL4-3 or pMSMnG were washed and lysed
637 in 1× NuPAGE LDS sample buffer (NP0007, Thermo Fisher Scientific) containing 2% (v/v) β-
638 mercaptoethanol and incubated at 70 °C for 10 m. For protein detection, the following antibodies were
639 used: mouse anti-HIV-1 p24 monoclonal antibody (1:2,000, clone 183-H12-5C, ARP-3537, obtained
640 from the HIV Reagent Program, NIH)[66], horseradish peroxidase (HRP)-conjugated goat anti-mouse

641 IgG antibody (1:20,000, 074-1806, KPL) and HRP-conjugated horse anti-mouse IgG antibody
642 (1:2,000, A3854-200UL, Sigma-Aldrich). Chemiluminescence was detected using Western BLoT
643 Ultra Sensitive HRP Substrate (T7104A, Takara) according to the manufacturer's instruction. Bands
644 were visualized using an iBright FL1500 Imaging System (Thermo Fisher Scientific), and the band
645 intensity was quantified using iBright Analysis Software v5.2 (Thermo Fisher Scientific). Band
646 intensities are presented as values relative to those without ZCCHC3.
647
648 ***Purification of recombinant protein***
649 Plasmids encoding hexahistidine (Hisx6)- and glutathione S-transferase (GST)-tagged proteins were
650 introduced into *Escherichia coli* strain BL21(DE3) CondonPlus RIL (230245, Agilent Technologies,
651 Inc.), and the expression of the recombinant protein was induced by 0.5 mM isopropylthio-β-D-
652 galactoside (IPTG) in Luria Bertani broth at 18 ℃ for 6 h. The Hisx6-fused protein was purified from
653 the cell lysate by Ni-NTA column (141-09764, Fujifilm, Tokyo, Japan) and dialyzed by 200 mM NaCl,
654 50 mM HEPES, 1 mM 2-mercaproethanol for 6 h at 4 ℃. The GST-fused proteins were purified by
655 Glutathione Sepharose 4B-column (17127901, Cytiva) and dialyzed by 200 mM NaCl, 50 mM HEPES,
656 7:100000 (V/V) β-mercaptoethanol (99%) for 6 h at 4 ℃. The proteins were concentrated by Amicon
657 Ultra (M.W. 3,000 Da) (Sigma-Aldrich) and stored at -80 ℃.
658
659 ***Protein Pull-down assay***
660 HEK293T cells were cultured in DMEM to 80% confluency, harvested by centrifugation at 500 g for
661 3 min, and re-suspended with PBS (pH 7.4) containing 1% (v/v) protease inhibitor cocktail (25955-11,
662 Nacalai Tesque, Kyoto, Japan) 0.25% (w/v) Triton X-100 and incubated on ice for 10 min. Insoluble
663 fraction was removed by centrifugation (1,500 g, 5 min), and the supernatant was collected. For pull-
664 down assay using GST-fusion proteins, the purified GST-tagged Gag fragments (~5 μg) were mixed
665 with the lysate of HEK293T cells expressing HA- or EGFP-tagged proteins (ZCCHC3 fragments) and

666 glutathione Sepharose™ 4B in Pull-down buffer (PBS (pH 7.4), 1 mM DTT), and incubated for 30
667 min at 25 °C with gentle rotation. The beads were washed, and the bound proteins were eluted with
668 200 mM glutathione in Pull-down buffer, mixed with SDS-PAGE sample buffer (100 mM Tris-HCl
669 (pH 6.8), 4% (w/v) SDS, 20% (v/v) glycerol, 0.15 mg/mL bromophenol blue), and heated for 5 min.
670 The proteins were analyzed by SDS-PAGE using 12% (w/v) acrylamide gel and subjected to western
671 blot. HA- and EGFP-tagged proteins were incubated with anti-HA antibody (1: 2,000; 2999, Cell
672 Signaling Technology, Danvers, MA, USA) or anti-EGFP antibody (1: 2,000; 598, Medical &
673 Biological Laboratories Co., Ltd., Nagano, Japan), followed by the incubation with secondary antibody
674 (HRP-conjugated goat anti-mouse antibody (1: 10,000; NA931V, Cytiva) or HRP-conjugated goat
675 anti-rabbit antibody (1: 10,000; A-11036, Thermo Fisher Scientific, Waltham, MA, USA). The
676 immunoreactive bands were visualized using Chemi-Lumi One Super Kit (Nacalai Tesque) under
677 LAS-3000 Imager (Fujifilm). The gel was also stained with Coomassie Brilliant Blue (CBB) to check
678 the input amount and the unbound fraction.
679
680 ***RNA and DNA pull-down***
681 GST-tagged proteins were immobilized to glutathione sepharose beads (Cytiva) and incubated with
682 synthesized RNA for 10 min in RNA Pull-down buffer (20 mM Tris-HCl (pH 7.4), 30 mM NaCl, 0.1
683 mM $MgCl_2$, 1 mM DTT, 1:100 RNase inhibitor (SIN-201, TOYOBO, CO., ltd., Osaka, Japan) in
684 RNase-free water). The protein-RNA complex was eluted with 200 mM glutathione in RNA Pull-
685 down buffer. The RNA amount in the eluted fraction was quantified with Quanti Fluor RNA dye
686 (E286A, Promega, Madison, WI, USA) by following the manufacturer's instruction. The eluted
687 fraction was also subjected to SDS-PAGE, followed by CBB staining. For DNA pull-down assay, the
688 DNA fragments were amplified by PCR using a plasmid carrying HIV-1 5′ LTR (454 - 634 nt,
689 GenBank: MN989412.1), MLV 5′ LTR (1 - 207 nt, GenBank: KU324804.1) or Gag (935 - 1115 nt,
690 GenBank: MN989412.1) as a template and the primers described in Supplementary Table 1. Single-

691 stranded DNAs were generated by heating the dsDNA at 95 °C for 5 min, and quickly chilled on ice.
692 The dsDNA and ssDNA were used in the pull-down assay instead of RNA as described above.
693
694 ***Immunofluorescence microscopy and confocal microscopy***
695 Cells were fixed with 4% (w/v) paraformaldehyde (PFA) in PBS (pH 8.0) for 15 min and incubated
696 with 5% (v/v) goat serum (Cedarlane, Burlington, ON, Canada), in PBS (pH 8.0) containing 0.25%
697 (w/v) TritonX-100 for 15 min. The following primary antibodies were used: anti-LSM14A rabbit
698 polyclonal antibody (1: 500; HPA017961, Atlas Antibodies, Stockholm, Sweden), anti-p24 mouse
699 monoclonal antibody (1: 500; MAB7360, R&D, Minneapolis, MN, USA) and anti-ZCCHC3 mouse
700 monoclonal antibody (1: 500; SAB1408147, Sigma-Aldrich). The following secondary antibodies
701 were used: Alexa Fluor-647 goat anti-mouse IgG (1: 1,000; ab150115, Abcam, Cambridge, UK),
702 Alexa Fluor-568 goat anti-rabbit IgG (1: 1,000; A-11036, Thermo Fisher Scientific) and Alexa Fluor-
703 488 goat anti-mouse IgG (1: 1,000; A-11034, Thermo Fisher Scientific, Waltham, MA, USA). Nuclei
704 were stained with DAPI. For the cells expressing fluorescence protein-tagged proteins, the cells were
705 fixed with 4% (w/v) PFA in PBS (pH 8.0) and stained with DAPI. The cells were observed using a
706 confocal laser scanning microscope (FV-3000, Olympus, Tokyo, Japan) with a 100x objective lens
707 (NA 1.42.). The obtained images were analyzed with ImageJ (v 1.52q, NIH, Bethesda, MD, USA). A
708 stage incubator (TOKAI HIT Corporation, Shizuoka, Japan) was used for live-cell imaging; all
709 observations were performed at 37 °C and 5.0% CO_2.
710
711 ***Purification of virus from culture medium by centrifugation***
712 Cells were separated from culture medium by low-speed centrifugation (700 g, 5 min, 4 °C). The cell
713 lysate was prepared as described in the previous section (Protein pull down assay). For concentrating
714 the virion from the culture medium, the medium was layered onto 20% (w/v) sucrose in PBS (pH 7.4)
715 layer and centrifuged at 20,380 g for 2 h at 4 °C. After removing the supernatant, the pellet was re-

716 suspended with ice-cold lysis buffer (PBS containing 1% (v/v) protease inhibitor cocktail (25955-11,
717 Nacalai Tesque) 0.25% (w/v) Triton X-100, pH 7.4). The lysates (cell and virus) were subjected to
718 SDS-PAGE (12% (w/v) acrylamide gel) and western blot analyses using anti-EGFP antibody (1:
719 2,000; A-11036, Medical & Biological Laboratories Co., Ltd.), anti-p24 antibody (1:500; MAB7360,
720 R&D), and anti-β actin antibody (1:5,000; A5441, Sigma-Aldrich).
721
722 ***Flow cytometry***
723 HeLa and TZM-bl cells were fixed with 4% (w/v) PFA in PBS (pH 8.0) for 15 min at 25 °C. The cells
724 were washed three times and re-suspended with PBS (pH 7.4). After filtration through nylon mesh, the
725 cells were analyzed by a flow cytometer (LSRFortessa, BD Biosciences or Attune CytPix Flow
726 Cytometer, Thermo Fisher Scientific). Data were analyzed using FlowJo software (vX). To confirm
727 the expression of HA-tagged ZCCHC3 and cGAS, the cell lysate was subjected to SDS-PAGE and
728 western blot analyses using anti-HA antibody (1:2,000, 2999S, Cell Signaling Technology).
729
730 ***p24 ELISA***
731 The culture medium of Lenti-X 293T or HEK293T cells were harvested and centrifuged at 1,500 g for
732 10 min to remove cell debris. The p24 amount in the medium was quantified by Lenti-X p24 Rapid
733 Titer Kit (632200, Takara Bio Inc.) with the p24 control samples, following the manufacturer's
734 instructions.
735
736 ***HiBiT assay***
737 For culture supernatant of Lenti-X 293T cells transfected with the psPAX2-IN/HiBiT plasmid, the
738 HiBiT value was measured 2 days after transfection using the Nano Glo HiBiT Lytic Detection System
739 (N3040, Promega) as described previously[51]. The HiBiT value was converted to p24 value based on a
740 standard curve generated with a HiBiT-containing lentiviral vector whose p24 level was already

741 determined by p24 ELISA.

742

743 ***Zcchc3 depletion***

744 To deplete *Zcchc3*, Lenti-X 293T cells adjusted to 1.25 × 10^6 cells per well in a 6-well plate were
745 transfected with TriFECTa® RNAi Kit (hs.Ri.ZCCHC3.13, REF#: 107099486, IDT, Coralville, IA,
746 USA) or non-targeting control siRNA with TransIT-X2 Dynamic Delivery System (V6100, Takara
747 Bio Inc.) in Opti-MEM. After overnight culture, the cells were re-plated on a new 96-well plate at 2.5
748 × 10^4 cells per well. The cells were cultured again overnight and subjected to the quantification of
749 mRNA by qRT-PCR using the CellAmp Direct RNA Prep Kit for RT-PCR (Real Time) (3732, Takara
750 Bio Inc.), One Step TB Green PrimeScript PLUS RT-PCR Kit (Perfect Real Time) (RR096A, Takara
751 Bio Inc.), and primer pairs for *Zcchc3* (5′-CTCTCTATGCCTTCTTAAACCGA-3′ and 5′-
752 CATCTGCACGCTACAGTTCT-3′) and *ACTB* (5′-ACAGAGCCTCGCCTTTG-3′ and 5′-C
753 CTTGCACATGCCGGA G-3′). qRT-PCR was performed using the QuantStudio 5 Real-Time PCR
754 System (Thermo Fisher Scientific), and the Ct values of *Zcchc3* were normalized to the mean values
755 obtained using *ACTB* as a housekeeping gene (ΔΔCt method).

756

757 ***Generation of Zcchc3 knockout cells***

758 LentiCRISPRv2 plasmids (52961, Addgene) targeting *Zcchc3* gene were generated as follows. The
759 following oligos (100 pmol) were mixed and heated at 95 °C for 5 min, followed by incubation at room
760 temperature for 1 h for annealing, with 5′-caccgCCTGTTCCTACGCGTCTACG-3′ and 5′-
761 aaacTAACCTCTCGGAGCCTCTGCc-3′ for sgRNA#1, and 5′-
762 caccgCCTGTTCCTACGCGTCTACG-3′ and 5′-aaacTAACCTCTCGGAGCCTC TGCc-3′ for
763 sgRNA#2. The mixture was 250-fold diluted with water and used for ligation with the lentiCRISPRv2
764 plasmid, which was predigested with Esp3I (R0734S, NEB). The solution was mixed with DNA
765 Ligation Kit <Mighty Mix> (6023, Takara Bio Inc.) and used for transformation with NEB 5-alpha

766 F′Iq Competent *E. coli* (High Efficiency) (C2992H, NEB, Ipswich, MA, USA). After the miniprep,
767 the nucleotide sequence of the plasmid was verified by nucleotide sequencing using a primer (5′-
768 GAGGGCCTATTTCCCATGATT-3′).
769 The lentiCRISPRv2-Zcchc3-sgRNA#1 or lentiCRISPRv2-Zcchc3-sgRNA#2 plasmids were used for
770 co-transfection with psPAX2-IN/HiBiT and pMD2.G plasmids on Lenti-X 293T cells using TransIT-
771 293 Transfection Reagent. The culture supernatant was collected 2 days after transfection and used for
772 infection on Lenti-X 293T cells. The cells were cultured for 2 weeks in the presence of 1 μg/mL
773 puromycin (ant-pr-1, InvivoGen). The cells were single-cell-cloned using a limiting dilution method.
774 Presence or absence of a ZCCHC3 specific band with each clone was determined by western blotting
775 using an anti-human ZCCHC3 antibody (SAB1408147, Sigma-Aldrich) .
776
777 ***Reverse Transcription quantitative PCR***
778 Lenti-X 293T cells were co-transfected with pNL4-3 with or without pCMV-HA-ZCCHC3 plasmid.
779 At 2 days after transfection, the total RNA was extracted from cells using an RNeasy Mini Kit (74104,
780 QIAGEN, Hilden, Germany) and QIAshredder (79656, QIAGEN,, Hilden, Germany), and subjected
781 to RT-qPCR for quantification with the primer pairs for Gag-coding region (5′-
782 TGTAATACCCATGTTTTCAGCA-3′ and 5′-TCTGGCCTGGTGCAATAGG-3′) and *ACTB* (5′-
783 TCCAAATATGAGATGCGTTGTT-3′ and 5′-TGCTATCACCTCCCCTGTGT-3′). The qPCR was
784 performed using the StepOne Plus Real-Time PCR System (Thermo Fisher Scientific). The Ct values
785 of Gag-coding region were normalized to the mean values obtained using *ACTB* as a housekeeping
786 gene (ΔΔCt method).
787 For quantifying lentiviral RNA in the virion released from the producer cells to the culture medium,
788 RNA was purified from the medium with NucleoSpin® RNA Virus kit (U0956A, Takara Bio Inc.) by
789 following the manufacture's instruction and subjected to RT-qPCR with the primer pairs for EGFP
790 (5′-CAAGCTGACCCTGAAGTTCATCTG-3′ and 5′-TTGAAGAAGTCGTGCTGCTTCATG-3′)

791 and U5-coding region (5′-TCTGGCTAACTAGGGAACCCACTG-3′ and 5′-
792 ACTGCTAGAGATTTTCCACACTGA C-3′). The PCR mix (15 ul) contained One step TB Green
793 RT-PCR kit (RR096A, Takara Bio Inc.), each primer, 2 μL of nucleic acid samples and water. The
794 primers were presented at a final concentration of 400 nM. The qPCR was performed using the
795 StepOne Plus Real-Time PCR System (Thermo Fisher Scientific).
796
797 ***Preparation of viral RNA***
798 The plasmid carrying HIV-1 5′ LTR (454 - 634 nt, GenBank: MN989412.1), MLV 5′ LTR (1 - 207 nt,
799 GenBank: KU324804.1), EIAV 5′ LTR (1 - 114 nt, GenBank: AF247394.1), SIV 5′ LTR (1 - 351 nt,
800 GenBank: DQ374657.1) and Gag (935 - 1115 nt, GenBank: MN989412.1) under T7 promotor was
801 linearized at the 3' end of the insert, and used as a template in *in vitro* transcription reaction
802 (MegaSscript T7 Transcription Kit (AM1333, Ambion, Waltham, MA, USA). The synthesized RNA
803 was purified by isopropanol precipitation and quantified by measuring OD 260 nm. Short stem-loop
804 RNA molecules derived from HIV-1 LTR (SL-1, 2, and 3) were synthesized by FasMac. The
805 sequences were as follows: SL1, 5'-
806 UCUCUGGUUAGACCAGAUCUGAGCCUGGGAGCUCUCUGGCUAACUAGGGA-3'; SL2, 5'-
807 CCACUGCUUAAGCCUCAAUAAAGCUUGCCUUGAGUGCUCAAAGUAGUGU-3'; and SL3,
808 5'-CUAGAGAUCCCUCAGA CCCUUUUAGUCAGUGUGGAAAAUCUCUAG-3'.
809
810 ***Electrophoretic mobility shift assay (EMSA)***
811 ssRNA, dsDNA and ssDNA were prepared as described in the previous section (RNA and DNA pull
812 down). Synthesized nucleic acids (0.1 pmol) were incubated with purified proteins (0, 0.1, 0.2, 1 pmol)
813 in EMSA binding buffer (40 mM Tris (pH 8.0), 2 mM KCl, 1 mM $MgCl_2$, 1% (w/v) NP-40, 1 mM
814 DTT in RNase-free water) at 25 °C for 10 min. The samples were separated by electrophoresis using
815 3.5% (w/v) acrylamide/bisacrylamide gel in TBE (100 mM Tris-base, 100 mM boric acid, 2 mM

816 EDTA), and visualized with SYBR™ Gold Nucleic Acid Gel Stain (S11494, Thermo Fisher Scientific).

817

818 ***Stable cell line generation and BioID analysis***

819 HEK293T cells were co-transfected with pDON-5neo-TurboID tagged ZCCHC3, pGP and pMD2.G
820 at the ratio of 2:1:1 by PEI. The culture medium was collected 48 hours after transfection, centrifuged
821 at 1,500 g for 10 min at 4 °C to remove cell debris, and added to the culture medium of HeLa cells.
822 G418 was added to the medium at a final concentration of 100 μg/mL 48 hours after infection. Cells
823 were diluted to a 96-well-plate at the concentration of 1 - 5 cells per well. Positive wells were screened
824 using a confocal laser scanning microscope (FV-3000, Olympus) The cells were infected by lentivirus
825 produced as described in the previous section (Plasmid transfection, virus production and collection,
826 virus infection) for 30 min before labelling. For labelling with biotin, the cells were incubated with
827 500 mM biotin for 30 min. The cells were rinsed with 5 mL ice-cold HEPES-saline (20 mM HEPES-
828 NaOH, pH 7.5, 137 mM NaCl). Another 2 mL HEPES-saline was added to the dish to collect the cells
829 with scraping. The cells were harvested by centrifugation at 800 g for 3 min at 4 °C and re-suspended
830 with 500 μL Guadinine-TCEP buffer (8 M Guadinine, 100 mM HEPES-NaOH, pH 7.5, 10 mM tris(2-
831 carboxyethyl)phosphine hydrochloride, 40 mM chloroacetamide). Proteins were extracted and
832 digested with trypsin followed by enrichment of biotinylated peptides as described previously[67]. LC-
833 MS/MS analysis of the biotinylated peptides was performed on an EASY-nLC 1200 UHPLC
834 connected to an Orbitrap Fusion mass spectrometer (Thermo Fisher Scientific) as described
835 previously[67]. Raw data were directly analyzed against the SwissProt database restricted to *Homo*
836 *sapiens* using Proteome Discoverer version 2.5 (Thermo Fisher Scientific) with Sequest HT search
837 engine. The search parameters were as follows: (a) trypsin as an enzyme with up to two missed
838 cleavages; (b) precursor mass tolerance of 10 ppm; (c) fragment mass tolerance of 0.6 Da; (d)
839 carbamidomethylation of cysteine as a fixed modification; and (e) acetylation of protein N-terminus,
840 oxidation of methionine, and biotinylation of lysine as variable modifications.

841

842 ***Luciferase assay***

843 Cells infected with a luciferase-encoding virus were lysed 2 days after infection with a Bright-Glo
844 Luciferase Assay System (E2620, Promega) and the luminescent signal was measured using a GloMax
845 Explorer Multimode Microplate Reader (Promega).

846

847 ***Statistics***

848 The total number of independent experiments in each analysis is described in the figure legends. All
849 statistical analyses were evaluated by an unpaired, two-tailed Student's *t*-test unless otherwise
850 indicated. $p \leq 0.05$ were considered statistically significant. The tests were performed using Prism 9
851 software v9.1.1 (GraphPad Software Inc., Boston, MA, USA).

852

853 ***Protein structure predictions***

854 The three-dimensional protein structure of human ZCCHC3 (NM_033089.7) was predicted using
855 ColabFold (v.1.5.2: AlphaFold2 using MMseqs2)
856 (https://colab.research.google.com/github/sokrypton/ColabFold/blob/main/AlphaFold2.ipynb).

857

858 ***Protein-RNA binding predictions***

859 The protein-RNA binding was predicted busing catRAPID omics (v2.0)
860 (http://s.tartaglialab.com/page/catrapid_omics2_group). The amino acids sequence of ZCCHC3, the
861 nucleotide sequences of HIV-1 LTR RU5 region and MLV LTR used for the prediction could be found
862 in NCBI (ZCCHC3: NM_033089.7; HIV-1 LTR RU5 region: MN989412.1; and MLV LTR:
863 KU324804.1).

864

865

866 **Data availability statement**

867 This study includes no original code deposited in external repositories. Source data are provided with
868 this paper. Any additional information required to reanalyze the data reported in this study is available
869 from the corresponding author upon request.

870

871 **Methods references**

872 [57] Adachi, A., et al. Production of acquired immunodeficiency syndrome-associated retrovirus in
873 human and nonhuman cells transfected with an infectious molecular clone. *J Virol.* **59**, 284–291
874 (1989).

875 [58] Keele, B.F., et al. Identification and characterization of transmitted and early founder virus
876 envelopes in primary HIV-1 infection. *Proc Natl Acad Sci U S A.* **105**, 7552–7557 (2018).

877 [59] Salazar-Gonzalez, J.F., et al. Genetic identity, biological phenotype, and evolutionary pathways
878 of transmitted/founder viruses in acute and early HIV-1 infection. *J Exp Med.* **206**, 1273–1289
879 (2009).

880 [60] Takehisa, J., et al. Generation of infectious molecular clones of simian immunodeficiency virus
881 from fecal consensus sequences of wild chimpanzees. *J Virol.* **81**, 7463–7475 (2007).

882 [61] Ozono, S., Zhang, Y., Tobiume, M., Kishigami, S. & Tokunaga, K. Super-rapid quantitation of
883 the production of HIV-1 harboring a luminescent peptide tag. *J Biol Chem.* **295**, 13023–13030
884 (2020).

885 [62] Ohishi, M., Shioda, T. & Sakuragi, J. Retro-transduction by virus pseudotyped with glycoprotein
886 of vesicular stomatitis virus. *Virology* **362**, 131–138 (2007).

887 [63] Sanjana, N.E., Shalem, O. & Zhang, F. Improved vectors and genome-wide libraries for CRISPR
888 screening. *Nat methods.* **11**, 783–784 (2014).

889 [64] Enomoto, M., Bunge, M.B. & Tsoulfas, P. A multifunctional neurotrophin with reduced affinity
890 to p75NTR enhances transplanted Schwann cell survival and axon growth after spinal cord injury.

891 *Exp Neurol.* **248**, 170–182 (2013).

892 [65] Morizako, N., et al. Generation of a bovine cell line for gene engineering using an HIV-1-based
893 lentiviral vector. *Sci Rep.* **12**, 16952 (2022).

894 [66] Park, S., et al. HIV-1 protease inhibitors slow HPV16-driven cell proliferation through targeted
895 depletion of viral E6 and E7 oncoproteins. *Cancers* **13**, 949 (2021)

896 [67] Nishino, K., Yoshikawa, H., Motani, K. & Kosako, H. Optimized workflow for enrichment and
897 identification of biotinylated peptides using Tamavidin 2-REV for BioID and cell surface
898 proteomics. *J Proteome Res.* **21**, 2094–2103 (2022).

899

900

901

902 ***Acknowledgements***

903 The following reagents were obtained through the NIH HIV Reagent Program, Division of AIDS,
904 NIAID, NIH: Anti-Human Immunodeficiency Virus 1 (HIV-1) p24 Monoclonal (183-H12-5C), ARP-
905 3537, contributed by Dr. Bruce Chesebro and Kathy Wehrly. This research was supported by Japan
906 Agency for Medical Research and Development (AMED) under grants JP22fk0410033 (to A.S.),
907 JP21fk0108465 (to A.S.), JP22jk0210039 (to A.S.), JP22wm0325009 (to A.S. and S.H.Y.) and
908 JP22fk0410047 (to A.S. and S.H.Y.); JSPS Grants-in-Aid for Scientific Research on Innovative Areas
909 (19H04830 to S.H.Y.), JSPS Grant-in-Aid for Scientific Research (A) (23H00369 to S.H.Y.), JSPS
910 Grant-in-Aid for Scientific Research (C) (19K06382 to A.S.), and JSPS Grant-in-Aid for Scientific
911 Research (B) (22H02500 to A.S.); The Ito Foundation Research Grant R4 (to A.S.); Grant for Joint
912 Research Projects of the Research Institute for Microbial Diseases, Osaka University (to A.S.); and
913 the Joint Usage and Joint Research Programs, Institute of Advanced Medical Sciences, Tokushima
914 University (to H.K. and S.H.Y.). We thank S. Dodo, Y. Shibatani, T. Nishiuchi, M. Kumeta, Y. Yu,
915 and A. Jimpo for technical assistance.

916

917 ***Author contributions***

918 Experiments were designed by B.Y., A.S., J.L., P.S., and S.H.Y. Plasmids construction, recombinant
919 protein purification, protein pull-down assay, RNA pull-down assay, EMSA, RNA preparation,
920 reverse transcription quantitative PCR, and stable cell generation were performed by B.Y. and P.S.
921 Cell culture and transfection, confocal fluorescence microscopy, flow cytometry was performed by
922 B.Y., Y.L.T., E.P.B., S.H.Y., and A.S. BioID assay was performed by B.Y. and H.K. ZCCHC3
923 knockout cells generation and HiBiT assay were performed by Y.L.T. and A.S. Data analysis was
924 completed by B.Y., S.H.Y., and A.S. Manuscript writing, figure design, and editing was done by B.Y.,
925 H.K. S.H.Y and A.S. S.H.Y and A.S. supervised and funded the project.

926

927 ***Competing interest***

928 The authors declare that they have no conflict of interest.

929

930 ***Additional information***

931 Supplementary Information is available for this paper.

932 Correspondence and requests for materials should be addressed to Akatsuki Saito and Shige H.

933 Yoshimura.

934 Reprints and permissions information is available at www.nature.com/reprints.

935

936

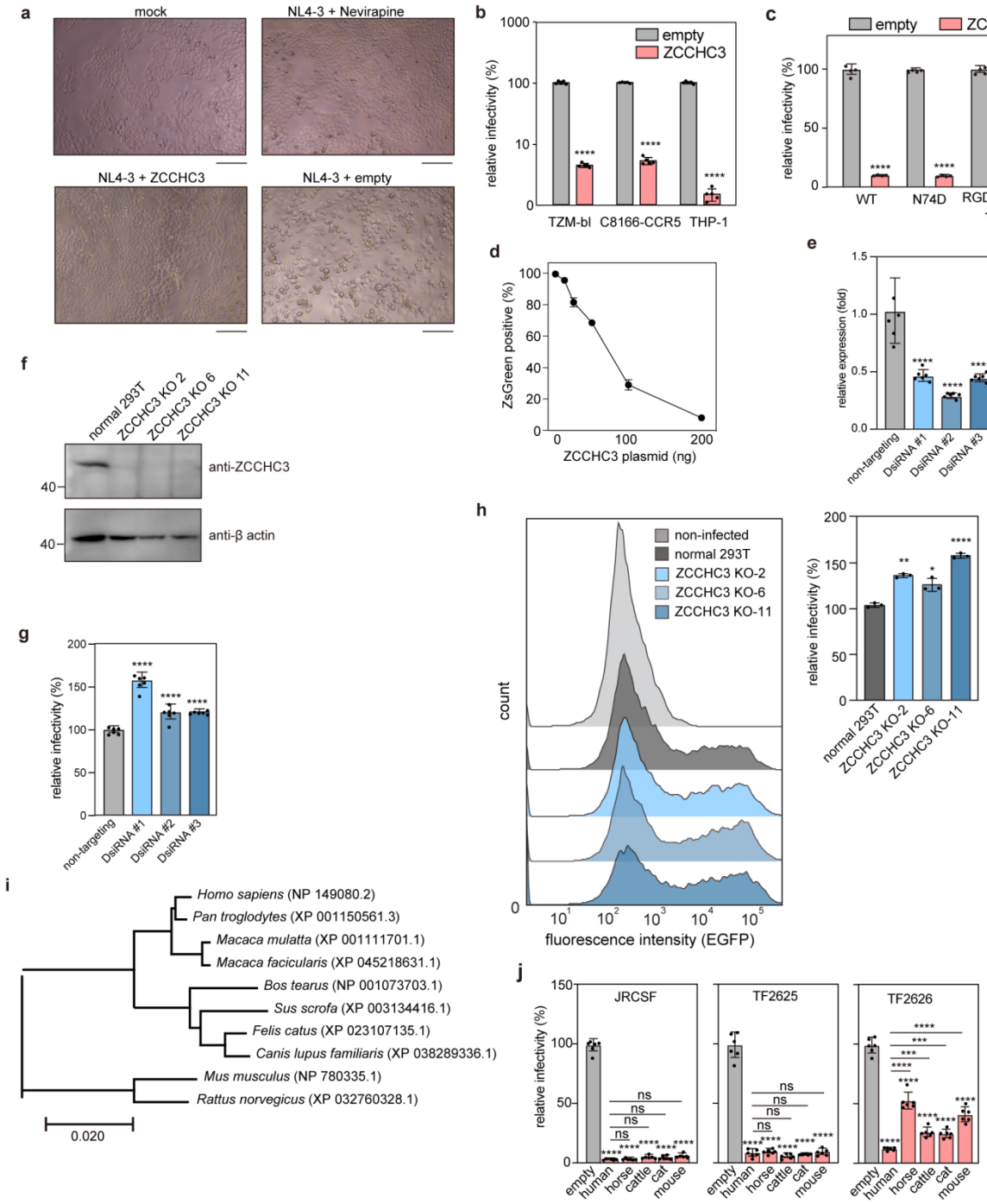

Extended Data Fig. 1| Additional data on the effect of ZCCHC3 on viral infection. a, TZM-bl cells were infected with NL4-3 viruses produced in the presence or absence of a HA-ZCCHC3 expression plasmid. The cells were observed by an optical microscopy 2 days after infection. TZM-bl cells infected with NL4-3 in the presence of Nevirapine served as a control (n =1). Scale bar, 50 µm. **b**, Antiviral effect of ZCCHC3 is Env-independent. pMSMnG plasmid was introduced into Lenti-X 293T cells with or without a ZCCHC3 expression plasmid. VSV-G-pseudotyped viruses were collected 2 days after transfection and used to infect the indicated cells. Infectivity on TZM-bl cells was determined as in (Fig. 1c); otherwise, it was determined by flow cytometry as a percentage of GFP-positive cells 2 days after infection. Values relative to those for cells harbouring empty vector are shown as the mean ± standard deviation (n = 5). **c**, Sensitivity of CA mutants to ZCCHC3. pMSMnG plasmid encoding the indicated

HIV-1 CA variant was introduced into Lenti-X 293T cells with or without a ZCCHC3 expression plasmid. Culture supernatant was collected 2 days after transfection and used to infect C8166-CCR5 cells. Infectivity was determined by flow cytometry as in (Extended Data Fig. 1b). Values relative to those for cells harbouring empty vector are shown as the mean ± standard deviation (n = 6). **d**, Dose-dependent suppression of lentiviral infectivity by ZCCHC3. Lenti-X 293T cells were co-transfected with EGFP-expressing lentiviral vectors together with different amounts of HA-ZCCHC3 expression vector. Culture supernatant was collected 2 days after transfection and used to infect MT-4 cells. Cell fluorescence was measured by flow cytometry 2 days after infection. The mean and standard deviation values from quadruplicate measurements are shown. **e**, Knock down of *Zcchc3*. *Zcchc3* mRNA in Lenti-X 293T cells transfected with DsiRNA targeting *Zcchc3* or control DsiRNA was quantified by RT-qPCR. The mean and standard deviation values are shown (n = 6). **f**, Western blot analysis of ZCCHC3-KO cells. Three KO cell lines were analyzed by western blotting using an anti-ZCCHC3 antibody, with β-actin as a loading control. A representative image from three independent experiments is shown. **g**, Effect of *Zcchc3* knockdown on viral infectivity on target cells. Lenti-X 293T cells transfected with DsiRNA targeting *Zcchc3* or control DsiRNA were infected with a lentiviral vector encoding the luciferase reporter protein. Infectivity was quantified as relative light units of luciferase and is presented as the mean and standard deviation (n = 6). **h**, Infectivity of lentivirus produced from normal and ZCCHC3-KO cells, analyzed by flow cytometry (left). Positive cells were counted (right). The mean and standard deviation values are shown from three independent experiments. **i**, Phylogenetic tree of mammalian ZCCHC3 proteins. The tree was constructed using the maximum-likelihood method. **j**, Anti-HIV-1 effect of mammalian ZCCHC3. A plasmid encoding the indicated virus was introduced into Lenti-X 293T cells with or without mammalian HA-ZCCHC3 expression plasmid. Culture supernatant was prepared, and TZM-bl cells infected and analyzed as in (Fig. 1**c**). Values relative to that of human ZCCHC3 are shown as the mean and standard deviation (n = 6). In **b**,**c**,**h**, differences were examined by a two-tailed, unpaired Student's *t*-test; ****$p < 0.0001$, **$p < 0.01$, *$p < 0.05$. In **e**,**g** and **j** differences were examined by one-way ANOVA, followed by Tukey's test; ****$p < 0.0001$, ***$p < 0.001$, ns $p < 0.01$.

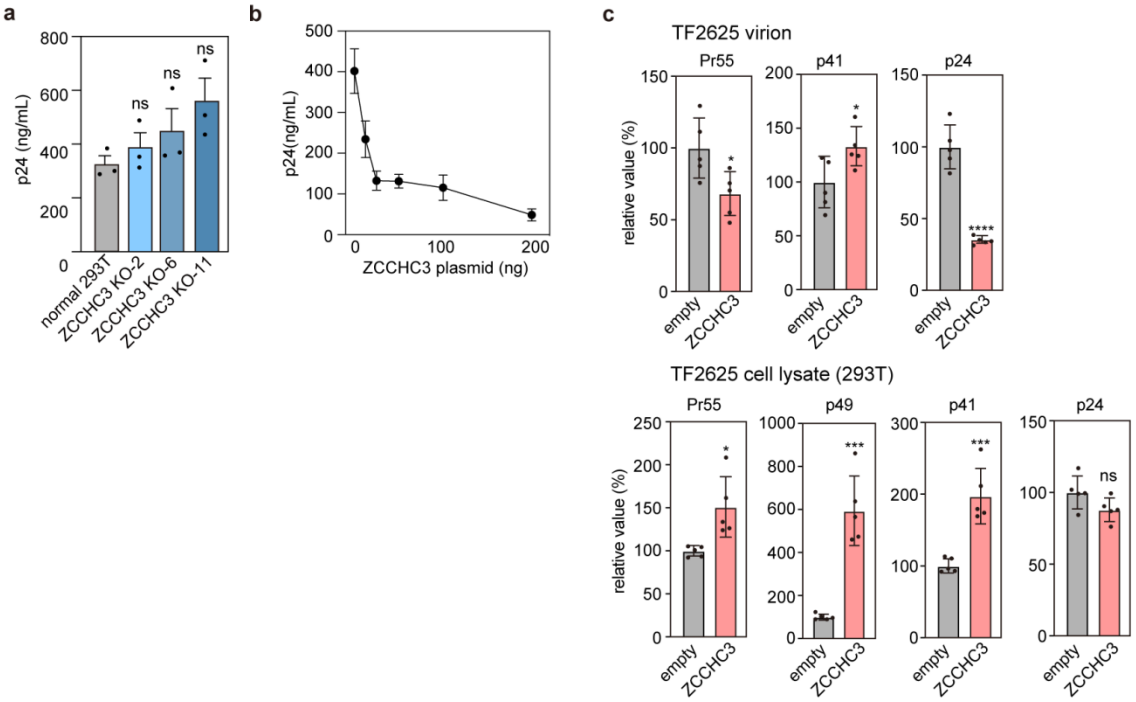

Extended Data Fig. 2| Additional data on the effect of ZCCHC3 on viral production. a,**b**, The amount of HIV-1 released into the culture medium described in Extended Data Fig. 1h (**a**) and Extended Data Fig. 1c (**b**), quantified by p24 ELISA. The mean and standard deviation values from three independent experiments are shown. **c**, Quantified band intensity from blots shown in Fig. 2b. Relative intensity of pr55, p49, p41, and p24 bands in the virion lysate (upper), or pr55, p49, p41, and p24 bands in the cell lysate (lower) of pTF2625-transfected cells was compared in the presence or absence of ZCCHC3 during virion production (n = 5). In **a**,**c**, differences were examined by a two-tailed, unpaired Student's *t*-test. ****$p < 0.0001$, ***$p < 0.001$, *$p < 0.05$; ns, $p \geq 0.05$.

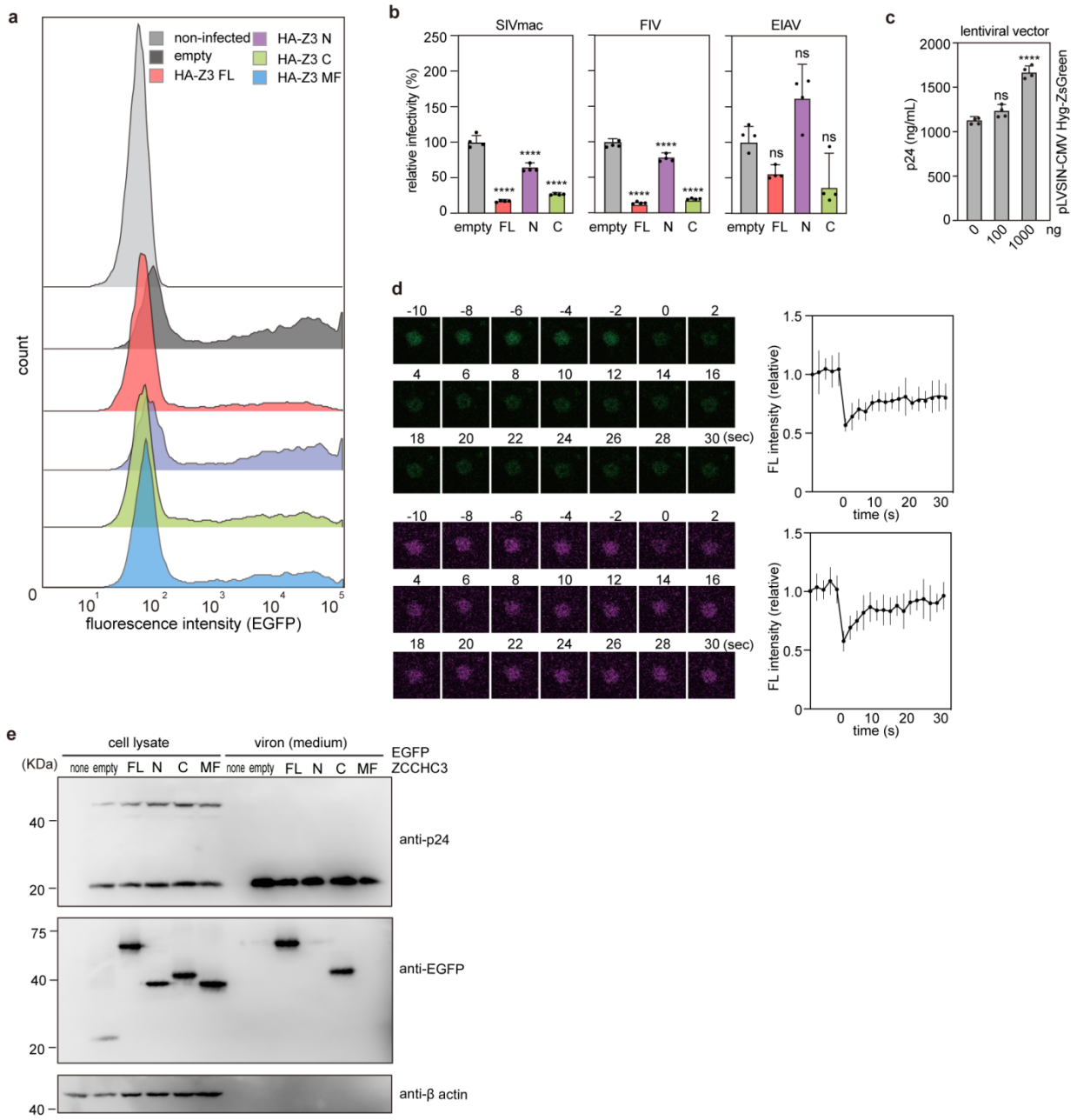

Extended Data Fig. 3| Additional data on ZCCHC3 binding to GagNC via C-terminal ZnFs. a, Changes of lentiviral infectivity upon ZCCHC3 loading. HeLa cells were infected with a p24-normalized amount of lentiviruses carrying a ZCCHC3 fragment (FL, N, C, or MF). Infectivity was analyzed based on the expression of a viral gene (EGFP) using flow cytometry. **b**, ZCCHC3 C fragment suppresses retroviral infection. Lenti-X 293T cells were co-transfected with plasmids for generating SIVmac, FIV, or EIAV lentiviral vectors in the presence of a ZCCHC3 fragment (FL, N, or C), and the resultant viruses were used to infect MT-4 cells. Infectivity was determined as relative light units 2 days after infection. Values relative to those of cells without ZCCHC3 expression are shown as the mean ± standard deviation (n = 5). **c**, Lenti-X 293T cells were co-transfected with 1000 ng of psPAX2-IN/HiBiT plasmid and different amounts of pLVSIN-CMV Hyg-ZsGreen vector. p24 concentration (converted from HiBiT value) in the culture supernatant was determined 2 days after transfection. Values are shown as the mean ± standard deviation (n = 4). **d**, FRAP analysis of a condensate formed by HIV-1 Gag NCp7 in HeLa cells. The foci were bleached, and

992 the fluorescence intensity in the area was measured. Data are shown as the mean (bold solid line) and standard
993 deviation (vertical lines) (n = 10). **e**, Incorporation of different ZCCHC3 fragments into the lentiviral virion. A
994 plasmid encoding EGFP-tagged ZCCHC3 FL, N, C, or MF was introduced into HEK293T cells together with
995 lentiviral plasmids (pLV-SIN-Hyg, psPAX2, pMD2.G). Virions released into the culture medium were harvested by
996 centrifugation and analyzed by immunoblotting with anti-GFP, anti-p24, and anti-β-actin antibodies. In **b**,**c**,
997 differences were examined by one-way ANOVA, followed by Tukey's test. ****$p < 0.0001$; ns, $p \geq 0.05$.
998

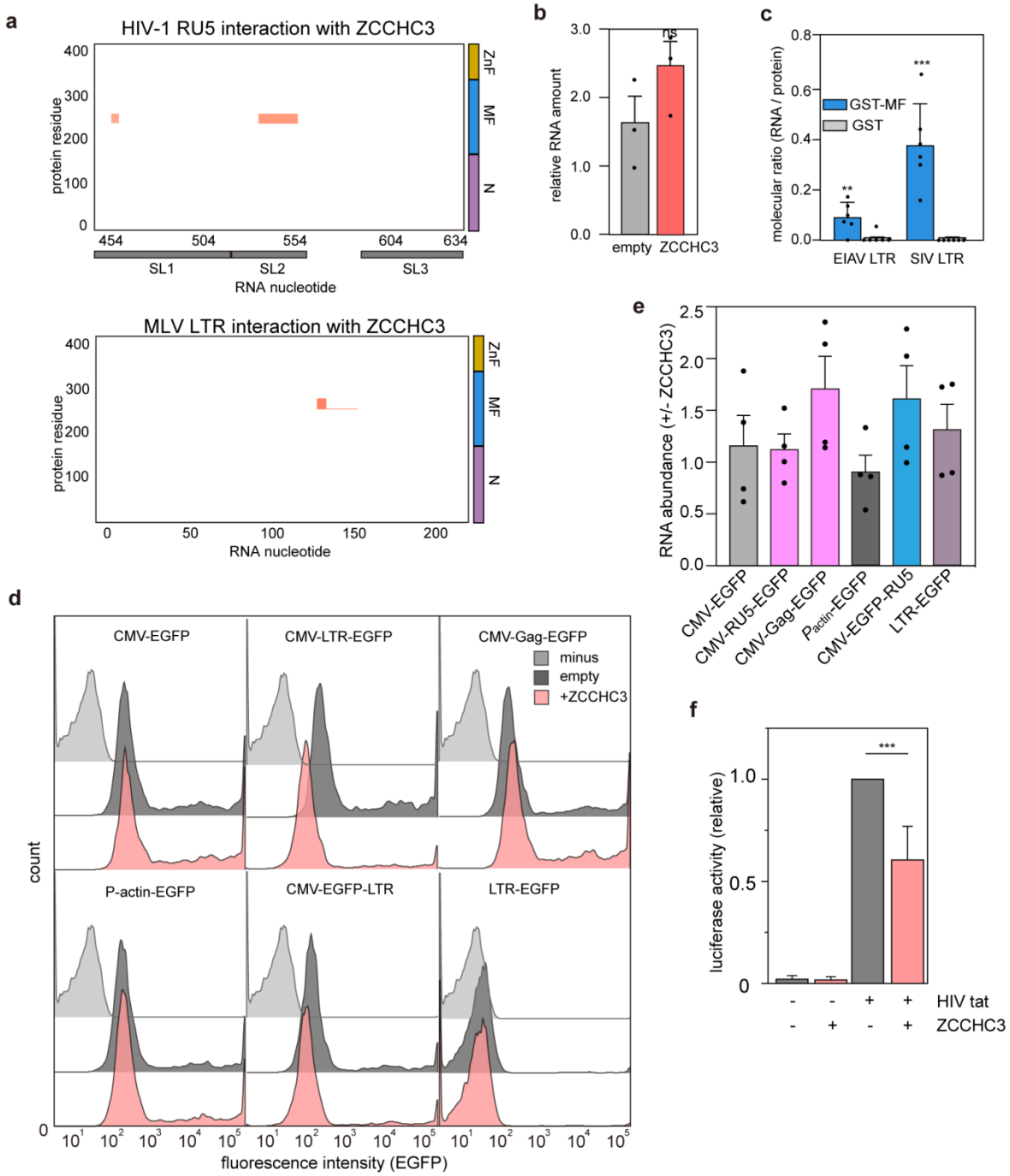

Extended Data Fig. 4| Additional data on ZCCHC3 binding to retroviral RNA. a, Binding propensity of ZCCHC3 to HIV1-1 LTR (R-U5) RNA sequence and MLV LTR sequence, predicted by catRAPID. The nucleotide numbers of HIV-1 (GenBank: MN989412.1) and MLV genomes (GenBank: KU324804.1) are plotted on the x-axis. The HIV-1 SL1, SL2, and SL3 positions are depicted along the x-axis. ZCCHC3 N, MF, and ZnF positions are depicted along the y-axis. **b**, Effect of ZCCHC3 on the expression of viral genes. pNL4-3 plasmid was introduced into Lenti-X 293T cells together with a vector encoding HA-ZCCHC3. Total RNA was purified, and viral RNA was quantified by RT-qPCR and normalized to β-actin mRNA expression level. The mean and standard deviation from three independent experiments are shown. **c**, ZCCHC3 MF domain binding to EIAV and SIV LTR RNA. RNA pull-down assay was performed using the ZCCHC3 MF fragment and EIAV LTR and SIV LTR, as in Fig. 4b. The mean

1009 and standard deviation values from three independent experiments. **d**. Representative traces of the reporter genes
1010 expression level (Fig. 5g). **f**, Effect of ZCCHC3 on viral gene expression in a proviral state. TZM-bl cells carrying
1011 a luciferase gene flanked by 5′- and 3′-LTRs were transfected with a plasmid encoding HIV-1 Tat with or without
1012 HA-ZCCHC3. Luciferase activity in the cell lysate was then measured. The data are presented as the mean ± standard
1013 deviation from four independent experiments. In **b–d** and **f,** differences were examined by a two-tailed, unpaired
1014 Student's *t*-test. ***$p < 0.001$, **$p < 0.01$, *$p < 0.05$; ns, $p \geq 0.05$.
1015

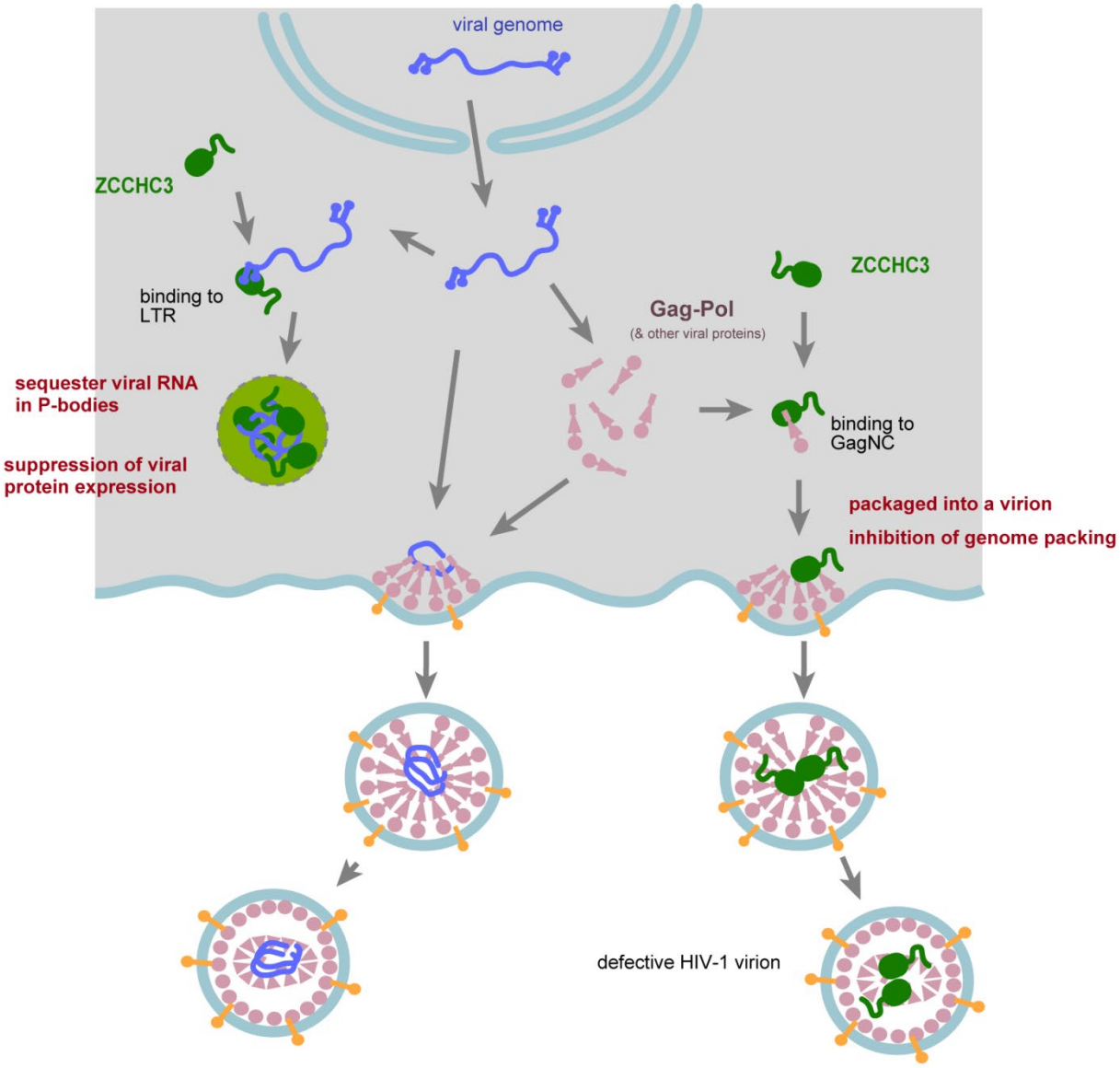

1016

1017 **Extended Data Fig. 5. Proposed mechanism of HIV-1 suppression by ZCCHC3.** The 5′ LTR region of nuclear-
1018 exported HIV-1 genomic RNA is recognised by the ZCCHC3 MF, and sequestered in the P-bodies, which impairs
1019 virion maturation. ZCCHC3 also binds to HIV-1 Gag NCp7, which leads to ZCCHC3 incorporation into the virion
1020 and promotes the antiviral function of ZCCHC3 during subsequent infection.

1021